Alexandria Engineering Journal (2020) xxx, xxx–xxx

HOSTED BY

Alexandria University

Alexandria Engineering Journal

www.elsevier.com/locate/aej
www.sciencedirect.com

New Caputo-Fabrizio fractional order $SEIAS_qE_qHR$ model for COVID-19 epidemic transmission with genetic algorithm based control strategy

M. Higazy [a,b,*], Maryam Ahmed Alyami [c]

[a] Department of Mathematics and Statistics, Faculty of Science, Taif University, Saudi Arabia
[b] Department of Physics and Engineering Mathematics, Faculty of Electronic engineering, Menoufia University, Menouf, Egypt
[c] Department of Mathematics, Faculty of Sciences, University of Jeddah, Jeddah, Saudi Arabia

Received 29 June 2020; revised 16 August 2020; accepted 24 August 2020

KEYWORDS

COVID-19;
Fractional derivative;
Caputo-Fabrizio fractional order differential operator;
The existence and uniqueness;
Genetic algorithm

Abstract Fractional derivative has a memory and non-localization features that make it very useful in modelling epidemics' transition. The kernel of Caputo-Fabrizio fractional derivative has many features such as non-singularity, non-locality and an exponential form. Therefore, it is preferred for modeling disease spreading systems. In this work, we suggest to formulate COVID-19 epidemic transmission via $SEIAS_qE_qHR$ paradigm using the Caputo-Fabrizio fractional derivation method. In the suggested fractional order COVID-19 $SEIAS_qE_qHR$ paradigm, the impact of changing quarantining and contact rates are examined. The stability of the proposed fractional order COVID-19 $SEIAS_qE_qHR$ paradigm is studied and a parametric rule for the fundamental reproduction number formula is given. The existence and uniqueness of stable solution of the proposed fractional order COVID-19 $SEIAS_qE_qHR$ paradigm are proved. Since the genetic algorithm is a common powerful optimization method, we propose an optimum control strategy based on the genetic algorithm. By this strategy, the peak values of the infected population classes are to be minimized. The results show that the proposed fractional model is epidemiologically well-posed and is a proper elect.

1. Introduction

COVID-19, the 2019 new corona-virus, 2019-nCoV or corona-virus of Wuhan are all names of the same transmissible virus causing respiratory contagion and highly transferred between humans. Until now, no one surely knows about the true source of COVID-19. The obvious truth is the existence of COVID-19

* Corresponding author.
E-mail address: m.higazy@tu.edu.sa (M. Higazy).
Peer review under responsibility of Faculty of Engineering, Alexandria University.

https://doi.org/10.1016/j.aej.2020.08.034

Please cite this article in press as: M. Higazy, M.A. Alyami, New Caputo-Fabrizio fractional order $SEIAS_qE_qHR$ model for COVID-19 epidemic transmission with genetic algorithm based control strategy, Alexandria Eng. J. (2020), https://doi.org/10.1016/j.aej.2020.08.034

between us, and the pain it causes to us every hour. The pain caused to us every hour is either because a new injury or the death of someone we know due to Covid-19. The most likely source of COVID-19 is a lack of respect for and transgression of the laws of nature. These irresponsible actions of humans have caused many similar disasters like that created by the "Severe Acute Respiratory Syndrome" (SARS) outset in China in 2003 [1], the "Middle East Respiratory Syndrome" (MERS) outset in Saudi Arabia in 2012 [2,3] and the MERS outset in South Korea in 2015 [4,5]. These epidemics have produced more than 8000 assured SARS patients and 2200 assured MERS patients, [6].

COVID-19 pandemic caused many losses worldwide, in the other side it motivates researchers in all fields to search for the nature of this virus, the way it spread, the symptoms it causes, how to deal with it, ultimately treat it permanently and prepare a vaccine for future prevention.

As realized by the WHO [7], mathematical models, mainly those that are depending on a period of time, have a crucial function in assisting health decision-makers and policy-makers. So far, only a few mathematical models have been announced that explain the nature of the transmission of COVID-19. For example the model that illustrates the relationship between bats, hosts, reservoir and people; and the model done for computing underestimated COVID-19 cases [8,9]. In [10], Khan and Atangana studied COVID-19 via fractional order $SEIARM$-model. By applying Atangana-Balenau derivative, the effect of the seafood market M on the other population classes was studied. Other applications of Atangana-Balenau derivative can be found for example in [11–13]. In [14], Gao et al. produced a new ("bats, hosts, reservoir, people and COVID-19") nonlinear dynamical model that clear the dynamics of COVID-19 transition from the Bats to humans. Goa et al., in [15], studied the epidemic prediction for COVID-19 epidemic by utilizing (q-$HATM$). The recorded cases information were used to determine the number of unrecorded cases in Wuhan, China. In [16], the authors utilized the available data about COVID-19 to produce a comparative mathematical study in order to help the interested decision makers. They used HIV-COVID-19 general model to emulate the pandemic status in several countries. In [17], using the Italian data, Atangana presented several statistical graphs to clear out the nature of COVID-19 transition. Utilizing these results he constructed a new model in which the effect of lock-down was taken into account. Also, novel fractal-fractional operators were suggested and utilized to the proposed system. Via several numerical cases, the efficiency of the lock-down was proved. In [18], A new dynamical model of COVID-19 was proposed and studied with a nonlocal fractional derivative operator.

In [19], Higazy generalized the integer order SIDARTHE COVID-19 epidemic model, that constructed firstly in [20], via fractional derivative scheme. In addition, certain optimum control strategies were constructed.

In [21], Biao Tang et al. constructed the $SEIAS_qE_qHR$ paradigm in order to predict the dynamics of the novel coronavirus transmission via the ordinary differential equations. Several problems in the real world can be formulated utilizing fractional-order mathematical paradigms, for example see [22–36].

Optimal control methods have been used by many researchers to minimize the total number of cases in the infected population, see for example [19,37–39] and [59–61]. The control plans may be via giving treatments to the detected infected cases, giving vaccines to the uninfected people, decreasing the contact rate via social distances or isolation, and encouraging personal hygiene through educational programs, see for example [19,37,38,40] and the related references cited therein.

As fractional derivative has a memory feature that makes it very useful in modelling epidemics' transition [10,19,41–43], in the current research, we continue our study about modelling COVID-19 epidemic transition via fractional derivative schemes. We generalize the 8-dimensions COVID-19 $SEIAS_qE_qHR$ model given in [21] utilizing Caputo-Fabrizio fractional operator. The reason of utilizing the Caputo-Fabrizio fractional operator to COVID-19 new model is that it has many features such as their kernel has useful features such as non-singularity, non-locality and an exponential form, and by utilizing this operator, the crossover action in the studied model can be good characterized via this fractional derivative operator. In the suggested fractional order COVID-19 $SEIAS_qE_qHR$ paradigm, the impact of quarantining and contact rates are examined. The stability of the disease free equilibrium is studied and a new parametric rule for the fundamental reproduction number formula is given. The existence and uniqueness of stable solution for the proposed fractional order COVID-19 $SEIAS_qE_qHR$ paradigm are proved. Since the genetic algorithm is a common powerful optimization method [44], we propose an optimum control strategy based on the genetic algorithm, by which the optimum contact and quarantining rates can be estimated. By this strategy, the peak values of the infected population classes are to be minimized for the proposed fractional order COVID-19 $SEIAS_qE_qHR$ paradigm. Research concerning Caputo-Fabrizio derivative and their utilization in several models in engineering and science can be found for example in [45,46] and the related papers cited there.

The remaining parts of this paper are arranged as follows. Required basic notions about Caputo-Fabrizio fractional derivative will be recognized in Section 2. In Section 3, the suggested fractional order COVID-19 $SEIAS_qE_qHR$ paradigm is introduced. The stability of the proposed fractional order COVID-19 $SEIAS_qE_qHR$ paradigm will be discussed in Section 3.1. The existence and uniqueness of stable solution of the proposed Caputo-Fabrizio fractional order COVID-19 $SEIAS_qE_qHR$ paradigm will be examined and proved in Section 3.2. Numerical simulations and results discussion will be recorded in Section 4. Genetic algorithm based three control examples of the proposed fractional order COVID-19 $SEIAS_qE_qHR$ paradigm will be presented in Section 5. The concluding words will be recorded in Section 6.

2. Required basic notions

Caputo's definition of the fractional derivative doesn't always describe the memory impact of the real time systems, this is because the kernel uniqueness in the Caputo concept of the fractional derivative [47]. In [48,49], another definition of the fractional differential operator in their kernel with no singularity was proposed by Caputo and Fabrizio. In the new definition, the kernel takes an exponential form. The derivation of the new Caputo-Fabrizio fractional differential operator was made in [50] by Losada and Nieto. The basic concepts and

Please cite this article in press as: M. Higazy, M.A. Alyami, New Caputo-Fabrizio fractional order $SEIAS_qE_qHR$ model for COVID-19 epidemic transmission with genetic algorithm based control strategy, Alexandria Eng. J. (2020), https://doi.org/10.1016/j.aej.2020.08.034

required properties for the studied model are displayed in the remaining part of this section.

Definition 2.1. Let $\psi \in K(l,u)$, $u > l$, $\rho \in [0,1]$. Caputo-Fabrizio derivative for arbitrary takes the form

$$\left(\Delta_t^{\rho}\right)\psi(t) = \frac{N(\rho)}{1-\rho}\int_l^t \frac{d\psi(t)}{dt} e^{-\left(\rho\frac{t-y}{1-\rho}\right)} dy$$

where $N(\rho)$ is the function normalization such that $N(0) = N(1) = 1$.

If the function $\varphi \notin K(l,u)$, the definition takes the form.

$$\left(\Delta_t^{\rho}\right)\varphi(t) = \rho\frac{N(\rho)}{1-\rho}\int_l^t (\varphi(t)-\varphi(y))e^{-\left(\rho\frac{t-y}{1-\rho}\right)} dy$$

If $\frac{\rho}{1-\rho} = \varkappa \in [0,1]$, then the definition takes the form.

$$\left(\Delta_t^{\rho}\right)\psi(t) = \frac{\bar{N}(\varkappa)}{\varkappa}\int_l^t \psi'(t)e^{-\left(\frac{t-y}{\varkappa}\right)} dy,\ \bar{N}(0) = \bar{N}(\infty) = 1 \quad \text{and} \quad \lim_{\varkappa\to\infty}\frac{1}{\varkappa}e^{\frac{y-t}{\varkappa}} = \lambda(y-t).$$

Definition 2.2. Let $u > 0$, $\psi \in H_1(0,u)$ and $0 < \rho < 1$. The Caputo fractional differential operator takes the form

$${}^{C}\Delta_t^{\rho}\psi(t) = \frac{1}{\Gamma(1-\rho)}\int_0^t \frac{1}{(t-y)^{\rho}}\psi'(y)dy,\ t > 0.$$

Calculus in with fractional order and in specific Caputo definition of fractional order have several real applications, [48,49,47,50]. The kernel $(t-y)$ is changed for Caputo and Fabrizio in [51]. Then the form becomes

$${}^{CF}\Delta_t^{\rho}\psi(t) = \frac{(2-\rho)N(\rho)}{2(1-\rho)}\int_0^t \left(e^{-\frac{\rho}{1-\rho}(t-y)}\right)\psi'(y)dy,\ t > 0$$

where the normalization constant, $N(\rho)$, depends on ρ. The new kernel hasn't singular point at $t = y$.

3. COVID-19 mathematical model with Caputo-Fabrizio fractional differential operator

In [21], Biao Tang et al. constructed the $SEIAS_qE_qHR$ model (1) in order to predict the dynamics of the novel coronavirus transmission. This model is tested and its parameters are evaluated using the recorded real data from tenth to fifteenth of January 2020 of the recorded cases confirmed by laboratory of 2019-nCoV cases that recorded in China by the report of situation from World Health Organization (WHO), the National Commission of Health of China and the Commission of Health in City of Wuhan and Hubei county [52,53].

$$\begin{aligned}
S'(t) &= -(\beta c + cq(1-\beta))S(t)I(t) \\
&\quad - (\beta c + cq(1-\beta))\theta S(t)A(t) + \lambda S_q(t); \qquad (1)\\
E'(t) &= \beta c(1-q)S(t)I(t) + \beta c(1-q)\theta S(t)A(t) - \sigma E(t);\\
I'(t) &= \sigma l E(t) - (\delta_I + \alpha + \gamma_I)I(t);\\
A'(t) &= \sigma(1-l)E(t) - \gamma_A A(t);\\
S_q'(t) &= cq(1-\beta)S(t)I(t) + cq\theta(1-\beta)S(t)A(t) - \lambda S_q(t);\\
E_q'(t) &= \beta cqS(t)I(t) + \beta cq\theta S(t)A(t) - \delta_q E_q(t);\\
H'(t) &= \delta_I I(t) + \delta_q E_q(t) - (\alpha + \gamma_H)H(t);\\
R'(t) &= \gamma_I I(t) + \gamma_A A(t) + \gamma_H H(t).
\end{aligned}$$

The $(SEIAS_qE_qHR)$-model is a generalization of the famous "Susceptible-Exposed-Infectious-Recovered" (SEIR) compartmentalized paradigm relied on the functional progress of the epidemic, epidemiological situation between people and intervention measures (Fig. 1). The parameters of the model were evaluated for the assured recorded cases of COVID-19 in China mainland and were used to calculate the fundamental reproduction number formula of the disease transmission [21]. In [21], SEIR paradigm was generalized by estimating the impact of intervention actions, thorough closing off and quarantine in addition to treatment.

Here, the model is generalized utilizing the Caputo-Fabrizio fractional order differential operator and written in (2) as:

$$\begin{aligned}
{}^{CF}\Delta_t^{\rho_1}S(t) &= -(\beta c + cq(1-\beta))S(t)I(t) \\
&\quad - (\beta c + cq(1-\beta))\theta S(t)A(t) + \lambda S_q(t); \qquad (2)\\
{}^{CF}\Delta_t^{\rho_2}E(t) &= \beta c(1-q)S(t)I(t) + \beta c(1-q)\theta S(t)A(t) - \sigma E(t);\\
{}^{CF}\Delta_t^{\rho_3}I(t) &= \sigma l E(t) - (\delta_I + \alpha + \gamma_I)I(t);\\
{}^{CF}\Delta_t^{\rho_4}A(t) &= \sigma(1-l)E(t) - \gamma_A A(t);\\
{}^{CF}\Delta_t^{\rho_5}S_q(t) &= cq(1-\beta)S(t)I(t) + cq\theta(1-\beta)S(t)A(t) - \lambda S_q(t);\\
{}^{CF}\Delta_t^{\rho_6}E_q(t) &= \beta cqS(t)I(t) + \beta cq\theta S(t)A(t) - \delta_q E_q(t);\\
{}^{CF}\Delta_t^{\rho_7}H(t) &= \delta_I I(t) + \delta_q E_q(t) - (\alpha + \gamma_H)H(t);\\
{}^{CF}\Delta_t^{\rho_8}R(t) &= \gamma_I I(t) + \gamma_A A(t) + \gamma_H H(t).
\end{aligned}$$

In the fractional order $(SEIAS_qE_qHR)$-model, (S) symbolizes the susceptible compartment, (E) symbolizes the exposed compartment, (A) symbolizes the symptomless infected compartment, (I) symbolizes the symptomatic infected compartment, (H) symbolizes the hospitalized cases compartment, (R) symbolizes the recuperated cases compartment, (S_q) symbolizes the quarantined susceptible compartment and (E_q) symbolizes the quarantined exposed. Via tracing the people's contact, q portion of the exposed humans to the virus are quarantined. The quarantined humans are splitted into two compartments E_q or S_q according to the power of infection [54], however the second portion, $1-q$, who contains humans that lost from tracing the people's contact, are moved to E population compartment or remain in S population compartment. Assume that β be the probability of transmission and c be the rate of contact. Then, the isolated humans, if uninfected (or infected), moved into the population S_q (or E_q) with rate $(1-\beta)cq$ (or cq). Humans who are not isolated, if infected, will be put in the E compartment with rate $c(1-q)\beta$. The sick humans could be determined and hence quarantined at a rate δ_I and also due to recovery can be moved to the R population compartment. In our theoretical analysis, the fractional orders will be assumed to be $(0 < \rho_i < 1,\ i = 1,2,3,\ldots,8)$. The first-order derivatives in (1) is generalized by the fractional order Caputo-Fabrizio differential operator in order to obtain the proposed fractional order derivative model. The other model parameters are explained as follows.

$c$is the rate of Contact, β is the per contact transmission Probability, q is rate of quarantining the exposed humans, σ is rate of transition of exposed humans to the class of infected humans, λ is the rate of releasing the quarantined uninfected humans, l is the Probability of infected cases to have symptoms, δ_I is the rate of transition from the group of infected with symptoms to the isolated infected group, δ_q is The rate of transition from isolated exposed cases to the isolated

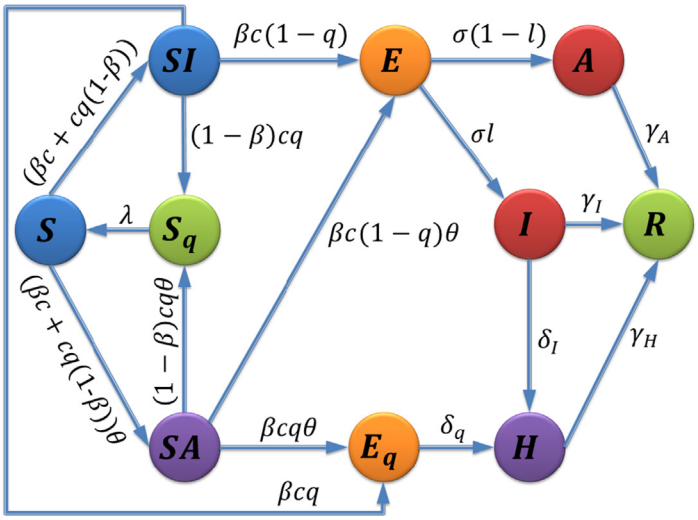

Fig. 1 ($SEIAS_qE_qHR$)-model's flow digraph $\mathscr{G}$.

infected group, γ_I is the rate of recovery of the group of infected with symptoms cases, γ_A is the rate of recovery of the symptomless infected cases, γ_H is the rate of recovery of isolated infected cases, θ is the rate of isolating the symptomless infected cases and α is the rate of death due to the disease. The computed values of the parameters in the model are recorded in the following table and taken from [21] and will be used later in the numerical simulations.

All states of the model (2) are positive and bounded with the initial conditions:

$$\begin{aligned} &S(0) = S(0) \geqslant 0;\ E(0) = E(0) \geqslant 0;\\ &I(0) = I(0) \geqslant 0;\ A(0) = A(0) \geqslant 0;\\ &S_q(0) = S_q(0) \geqslant 0;\ E_q(0) = E_q(0) \geqslant 0;\\ &H(0) = H(0) \geqslant 0;\ R(0) = R(0) \geqslant 0. \end{aligned} \tag{3}$$

By add up the eight equations of the model (2), the whole people's dynamics can be presented as follows.

$$D^{\rho}N(t) = -\alpha(H + I),$$

where $N(t) = S(t) + E(t) + I(t) + A(t) + S_q(t) + E_q(t) + H(t) + R(t)$.

The functional range for the studied model (2) is presented by

$$\Sigma = \left\{\left(S(t), E(t), I(t), A(t), S_q(t), E_q(t), H(t), R(t)\right) \in \mathbb{R}_+^8 : N(t) \leqslant N_{\max}\right\}.$$

3.1. Stability discussion of COVID-19 fractional order $SEIAS_qE_qHR$ model

The current subsection examines the stability for the fractional order COVID-19 $SEIAS_qE_qHR$ paradigm (2). The system has two equilibrium points, Disease Free Equilibrium (DFE) ($E_0 = (\overline{S}, 0, 0, 0, 0, 0, 0, 0)$) and the endemic equilibrium point (EEP) ($E_e = (S_e, E_e, I_e, A_e, S_{qe}, E_{qe}, H_e, R_e)$).

To show the behavior of the model, we divided it to three sub-systems: the first subsystem consists of the variable S which corresponds to susceptible class, the second subsystem consists of E, I, A, S_q, E_q and H (the infected people classes), that have non-zero values only during the transient time, and the third subsystem consists of the variable R (for the recovered class). The second infected classes subsystem, denoted as $EIAS_qE_qH$ subsystem. An remarkable notation is that the variables S and R are at equilibrium while (and only while) the infected individuals $E + I + A + S_q + E_q + H$ are zero. Variable R (which is monotonous increase) approaches to its asymptotic values $\overline{R}$, and S (which is monotonous decrease) approaches to $\overline{S}$ iff E, I, A, S_q, E_q and H approach to null.

The whole model can be reconstructed in a feedback scheme, wherever the $EIAS_qE_qH$ subsystem can be shown in a positive linear form with a feedback function f as following.

Define $\mathscr{I} = \left[EIAS_qE_qH\right]^{tr}$, we can reformate the $EIAS_qE_qH$ subsystem as:

$${}^{CF}\Delta_t^{\rho}X(t) = \mathscr{F}\mathscr{I}(t) + \mathscr{B}f(t) \tag{4}$$

$$= \begin{bmatrix} -\sigma & 0 & 0 & 0 & 0 & 0 \\ \sigma l & -\omega_1 & 0 & 0 & 0 & 0 \\ \omega_3 & 0 & -\gamma_A & 0 & 0 & 0 \\ 0 & 0 & 0 & -\lambda & 0 & 0 \\ 0 & 0 & 0 & 0 & -\delta_q & 0 \\ 0 & \delta_I & 0 & 0 & \delta_q & -\omega_2 \end{bmatrix} \mathscr{I}(t) + \begin{bmatrix} 1 & 0 & 0 \\ 0 & 0 & 0 \\ 0 & 0 & 0 \\ 0 & 1 & 0 \\ 0 & 0 & 1 \\ 0 & 0 & 0 \end{bmatrix} f(t)$$

$$Y_S(t) = [0 \quad \omega_4 \quad \theta\omega_4 \quad 0 \quad 0 \quad 0]\mathscr{I}(t) \tag{5}$$

$$Y_R(t) = [0 \quad \gamma_I \quad \gamma_A \quad 0 \quad 0 \quad \gamma_H]\mathscr{I}(t) \tag{6}$$

$$Y_f(t) = C\mathscr{I}(t) = \begin{bmatrix} 0 & \omega_5 & \theta\omega_5 & 0 & 0 & 0 \\ 0 & \omega_6 & \theta\omega_6 & 0 & 0 & 0 \\ 0 & \omega_7 & \theta\omega_7 & 0 & 0 & 0 \end{bmatrix} \mathscr{I}(t) \tag{7}$$

$$f(t) = S(t)\,Y_f(t) \tag{8}$$

where $\omega_1 = \delta_I + \alpha + \gamma_I, \omega_2 = \alpha + \gamma_H, \omega_3 = \sigma(1 - l), \omega_4 = \beta c + cq(1 - \beta)$, $\omega_5 = \beta c(1 - q), \omega_6 = cq(1 - \beta)$ and $\omega_7 = \beta cq$. The other state variables satisfy the following D.E.'s:

$${}^{CF}\Delta_t^{\rho}S(t) = -S(t)\,Y_S(t) + \lambda S_q(t) \tag{9}$$

$${}^{CF}\Delta_t^{\rho}R(t) = Y_R(t) \tag{10}$$

In view of the fact that the gain $S(t)$ of feedback finally approaches a constant value $\overline{S}$, it is possible to go ahead with parameters based analysis according to the limit feedback gain $\overline{S}$. The following result can be deduced.

Proposition 3.1. *The subsystem $EIAS_qE_qH$ is asymptotically stable with respect to susceptible group $\overline{S}$ iff $\overline{S} < S^*$ where*

$$S^* = \min\left\{ \begin{array}{c} \frac{\gamma_A(\sigma+\omega_1)+\sigma\omega_1}{l\sigma\omega_5+\theta\omega_3\omega_5}, \\ \frac{\gamma_A\sigma\omega_1}{(\gamma_A l\sigma\omega_5+\theta\omega_3\omega_5(\sigma+\omega_1)-\theta\sigma\omega_3\omega_5)}, \\ \frac{\sigma^2\omega_1+\sigma^2\gamma_A+\sigma\omega_1^2+2\sigma\omega_1\gamma_A+\sigma\gamma_A^2+\omega_1^2\gamma_A+\omega_1\gamma_A^2}{(l\omega_5\sigma^2+l\omega_5\sigma\omega_1+\theta\omega_3\omega_5\sigma+\theta\omega_3\omega_5\gamma_A)} \end{array} \right\} \tag{11}$$

Proof. Around the equilibrium DFE ($E_0 = (\overline{S}, 0, 0, 0, 0, 0, 0, 0)$), the Jacobian matrix will be as follows.

$$J(E_0) = \begin{bmatrix} 0 & 0 & -\omega_4\overline{S} & -\theta\omega_4\overline{S} & \lambda & 0 & 0 & 0 \\ 0 & -\sigma & \omega_5\overline{S} & \theta\omega_5\overline{S} & 0 & 0 & 0 & 0 \\ 0 & \sigma l & -\omega_1 & 0 & 0 & 0 & 0 & 0 \\ 0 & \omega_3 & 0 & -\gamma_A & 0 & 0 & 0 & 0 \\ 0 & 0 & \omega_6\overline{S} & \theta\omega_6\overline{S} & -\lambda & 0 & 0 & 0 \\ 0 & 0 & \omega_7\overline{S} & \theta\omega_7\overline{S} & 0 & -\delta_q & 0 & 0 \\ 0 & 0 & \delta_I & 0 & 0 & \delta_q & -\omega_2 & 0 \\ 0 & 0 & \gamma_I & \gamma_A & 0 & 0 & \gamma_H & 0 \end{bmatrix} \tag{12}$$

The matrix has two zero eigenvalues, and three negative real eigenvalues $\{-\omega_2, -\lambda, -\delta_q\}$, and three eigenvalues equal the roots of

$$\begin{aligned} P(\mu) &= b_0\mu^3 + b_1\mu^2 + b_2\mu + b_3 \\ &= D(\mu) - \overline{S}N(\mu) \end{aligned} \tag{13}$$

where

$$\begin{aligned} b_1 &= (\sigma+\omega_1+\gamma_A) \\ b_2 &= \left(\gamma_A(\sigma+\omega_1)+\sigma\omega_1-\overline{S}l\sigma\omega_5-\overline{S}\theta\omega_3\omega_5\right) \\ b_3 &= \left(\gamma_A(\sigma\omega_1-Sl\sigma\omega_5)-\overline{S}\theta\omega_3\omega_5(\sigma+\omega_1)+\overline{S}\theta\sigma\omega_3\omega_5\right) \\ D(\mu) &= \mu^3+(\sigma+\omega_1+\gamma_A)\mu^2+(\gamma_A(\sigma+\omega_1)+\sigma\omega_1)\mu+\gamma_A\sigma\omega_1 \\ N(\mu) &= (l\sigma\omega_5+\theta\omega_3\omega_5)\mu+\gamma_A l\sigma\omega_5+\theta\omega_3\omega_5(\sigma+\omega_1)-\theta\sigma\omega_3\omega_5) \end{aligned}$$

Applying Routh-Hurwiz stability criteria [55], the real parts of the eigenvalues of (13) will be negative if and only if all coefficients b_i of (13) are positive and $b_1b_2 - b_0b_3 > 0$. Then we have $b_1 > 0$,

$$\Rightarrow b_2 > 0 \tag{14}$$

$$\Rightarrow \overline{S} < \frac{\gamma_A(\sigma+\omega_1)+\sigma\omega_1}{l\sigma\omega_5+\theta\omega_3\omega_5}$$

$$\Rightarrow b_3 > 0 \tag{15}$$

$$\Rightarrow \overline{S} < \frac{\gamma_A\sigma\omega_1}{(\gamma_A l\sigma\omega_5+\theta\omega_3\omega_5(\sigma+\omega_1)-\theta\sigma\omega_3\omega_5)},$$

and

$$\Rightarrow b_1b_2 - b_0b_3 > 0, \tag{16}$$

$$\Rightarrow \overline{S} < \frac{\sigma^2\omega_1+\sigma^2\gamma_A+\sigma\omega_1^2+2\sigma\omega_1\gamma_A+\sigma\gamma_A^2+\omega_1^2\gamma_A+\omega_1\gamma_A^2}{(l\omega_5\sigma^2+l\omega_5\sigma\omega_1+\theta\omega_3\omega_5\sigma+\theta\omega_3\omega_5\gamma_A)}$$

From (14, 15, 16), we can deduce that (13) is Hurwitz (all real parts of the roots are negative) if and only if expression (11) satisfied. From (8), the transfer function between f and Y_f in the system (4)–(10) is $G(\mu) = N(\mu)/D(\mu)$ (13).

Due to the positive property of the system, the norm H_∞ of $G(\mu)$ equals to the static gain $G(0) = N(0)/D(0)$ [20]. Due to the observation come from [20], the basic reproduction

$$R_0 := \frac{1}{S^*} \tag{17}$$

and the equilibrium stability occurs when $SR_0 < 1$

In addition, remark that $R_0 = G(0)$ is the norm H_∞ of the transfer function $G(\mu)$ between f and Y_f in the system (4)–(10) [20]. □

The brink value S^* is of primary significance. Since, $S(t)$ approaches, asymptotically, monotonically to a limit $\overline{S}$, such a limit $\overline{S}$ must guarantee convergence of the $EIAS_qE_qH$ subsystem to zero (meaning stability; else, S could not reach $\overline{S}$). Subsequently, we can deduce the following proposition.

Proposition 3.2. *The limit value $\overline{S} = \lim_{t\to\infty} S(t) \leqslant S^*$ with positive initial conditions.*

Proof. Since $S(t)$ is non-negative and decreasing monotonically, which means that it has an end $\overline{S} \geqslant 0$. We can say that, after a proper large time t, it is clear that $S(t) \approx \overline{S}$. So, the system $SEIAS_qE_qHR$ acts equivalently to the linearized scheme related to the linearization in $\overline{S}$. Let us assume the contradiction case, $\overline{S}$ causes instability for this paradigm, then $\mathscr{I}(t)$ diverges, because the Metzler matrix $\mathscr{F} + \mathscr{B}\overline{S}C$ has a $+ve$ prevalent eigenvalue. Successively, that is mean that $\mathscr{I}(t)$ cannot reach to nil, therefore its ingredients stay positive, that is mean that $\omega_4 I(t) + \theta\omega_4 A(t) > 0$ does not reach to nil. As a result, ${}^{CF}\Delta_t^\rho S(t) = -S(t)(\omega_4 I(t) + \theta\omega_4 A(t)) + \lambda S_q(t) < 0$ also does not approach to nil, then $S(t)$ cannot approach to a non-negative limit $\overline{S} \geqslant 0$. a contradiction is obtained. □

The stability gate value S^* of Eq. (11) has a profound meaning. The value $\overline{S}$ is stand for the part of population that has not been infected at no time in the past or future. This limit is a decreasing function of the parameters $\beta, c, q, \theta$and l, that are the vital parameters. The act

$$f(t) = S(t)Y_f(t) = S(t)\begin{bmatrix} 0 & \omega_5 & \theta\omega_5 & 0 & 0 & 0 \\ 0 & \omega_6 & \theta\omega_6 & 0 & 0 & 0 \\ 0 & \omega_7 & \theta\omega_7 & 0 & 0 & 0 \end{bmatrix}\mathscr{I}(t) \tag{18}$$

has a destabilization effect of the under study subsystem $EIAS_qE_qH$, that would be steady in the absence this feedback. In order to save the stabilization of the subsystem $EIAS_qE_qH$ and confirm that the equilibrium $\overline{S}$ is approached, the coefficients of infection have to be little or the limit value $\overline{S}$ is little. Following [20], and from (17) the basic reproduction number of the system can be defined as:

$$R_0 := \frac{1}{S^*} = \frac{l\omega_5}{\omega_1} + \frac{\theta\omega_3\omega_5}{\gamma_A\omega_1} + \frac{\theta\omega_3\omega_5}{\gamma_A\sigma} - \frac{\theta\omega_3\omega_5}{\gamma_A\omega_1} \tag{19}$$

The stability of the DFE occurs while

$SR_0 < 1$

At the start of the epidemic, we have $S \simeq 1$ (100 % of the population) then the stability is reached while $R_0 < 1$.

3.2. Existence and uniqueness of solution for the fractional order ($SEIAS_qE_qHR$) system

In the current subsection, the solutions' existence and uniqueness (see [56]) for the Caputo-Fabrizio fractional order paradigm are studied taking into account the initial conditions of the system (2). By applying the operator of fractional Caputo-Fabrizio integral on the proposed studied model, we have

$$\begin{aligned}
S(t)-S(0) &= {}^{CF}I_t^{\rho_1}\left(-\omega_4 S(t)I(t)-\theta\omega_4 S(t)A(t)+\lambda S_q(t)\right); \quad (20)\\
E(t)-E(0) &= {}^{CF}I_t^{\rho_2}(\omega_5 S(t)I(t)+\theta\omega_5 S(t)A(t)-\sigma E(t);\\
I(t)-I(0) &= {}^{CF}I_t^{\rho_3}(\sigma lE-\omega_1 I);\\
A(t)-A(0) &= {}^{CF}I_t^{\rho_4}(\omega_3 E-\gamma_A A);\\
S_q(t)-S_q(0) &= {}^{CF}I_t^{\rho_5}\left(\omega_6 SI+\theta\omega_6 SA-\lambda S_q\right);\\
E_q(t)-E_q(0) &= {}^{CF}I_t^{\rho_6}\left(\omega_7 SI+\theta\omega_7 SA-\delta_q E_q\right);\\
H(t)-H(0) &= {}^{CF}I_t^{\rho_7}\left(\delta_I I+\delta_q E_q-\omega_2 H\right);\\
R(t)-R(0) &= {}^{CF}I_t^{\rho_8}(\gamma_I I+\gamma_A A+\gamma_H H).
\end{aligned}$$

Then, kernels take the form

$$\begin{aligned}
K_1(t,S) &= -\omega_4 S(t)I(t)-\theta\omega_4 S(t)A(t)+\lambda S_q(t); \quad (21)\\
K_2(t,E) &= \omega_5 S(t)I(t)+\theta\omega_5 S(t)A(t)-\sigma E(t);\\
K_3(t,I) &= \sigma lE-\omega_1 I;\\
K_4(t,A) &= \omega_3 E-\gamma_A A;\\
K_5\left(t,S_q\right) &= \omega_6 SI+\theta\omega_6 SA-\lambda S_q;\\
K_6\left(t,E_q\right) &= \omega_7 SI+\theta\omega_7 SA-\delta_q E_q;\\
K_7(t,H) &= \delta_I I+\delta_q E_q-\omega_2 H;\\
K_8(t,R) &= \gamma_I I+\gamma_A A+\gamma_H H.
\end{aligned}$$

It is known that the system states are positive functions according to the structure of the model i.e. $||S(t)|| \leqslant c_1$, $||E(t)|| \leqslant c_2$, $||I(t)|| \leqslant c_3$, $||A(t)|| \leqslant c_4$, $\left||S_q(t)|\right| \leqslant c_5$, $\left||E_q(t)|\right| \leqslant c_6$, $||H(t)|| \leqslant c_7$, $||R(t)|| \leqslant c_8$ where c_i $(i=1,2,\ldots,8)$ are certain non-negative constants. Let $\Omega(x)=\frac{2(1-x)}{(2-x)N(x)}$ and $\omega(x)=\frac{2x}{(2-x)N(x)}$. Denoting

$$\begin{aligned}
&\frac{\partial K_1}{\partial S}=\theta_1,\ \frac{\partial K_2}{\partial E}=\theta_2,\ \frac{\partial K_3}{\partial I}=\theta_3,\ \frac{\partial K_4}{\partial A}=\theta_4, \quad (22)\\
&\frac{\partial K_5}{\partial S_q}=\theta_5,\ \frac{\partial K_6}{\partial E_q}=\theta_6,\ \frac{\partial K_7}{\partial S}=\theta_7,\ \frac{\partial K_8}{\partial S}=\theta_8,
\end{aligned}$$

Applying Caputo-Fabrizio fractional integral to Eq. (20), we get

$$\begin{aligned}
S(t)-S(0) &= \Omega(\rho_1)K_1(t,S)+\omega(\rho_1)\int_0^t K_1(z,S)dz; \quad (23)\\
E(t)-E(0) &= \Omega(\rho_2)K_2(t,E)+\omega(\rho_2)\textstyle\int_0^t K_2(z,E)dz;\\
I(t)-I(0) &= \Omega(\rho_3)K_3(t,I)+\omega(\rho_3)\textstyle\int_0^t K_3(z,I)dz;\\
A(t)-A(0) &= \Omega(\rho_4)K_4(t,A)+\omega(\rho_4)\textstyle\int_0^t K_4(z,A)dz;\\
S_q(t)-S_q(0) &= \Omega(\rho_5)K_5\left(t,S_q\right)+\omega(\rho_5)\textstyle\int_0^t K_5\left(z,S_q\right)dz;\\
E_q(t)-E_q(0) &= \Omega(\rho_6)K_6\left(t,E_q\right)+\omega(\rho_6)\textstyle\int_0^t K_6\left(z,E_q\right)dz;\\
H(t)-H(0) &= \Omega(\rho_7)K_7(t,H)+\omega(\rho_7)\textstyle\int_0^t K_7(z,H)dz;\\
R(t)-R(0) &= \Omega(\rho_8)K_8(t,R)+\omega(\rho_8)\textstyle\int_0^t K_8(z,R)dz.
\end{aligned}$$

Theorem 3.3. *The kernels K_1; K_2; …; K_8 satisfy the conditions of Lipschitz and are contraction mappings if there exists $0 \leqslant U = \max\{\theta_i : i=1,2,\ldots,8\} < 1$.*

Proof. Consider the kernel K_i for any state variable X_i. Let X and X_1 be any two features.

$$\|K_1(t,S)-K_1(t,S_1)\| = \left\|\frac{\partial K_1}{\partial S}(S(t)-S_1(t))\right\| \quad (24)$$

Utilizing the triangle inequality on (24), we have

$$\begin{aligned}
\|K_1(t,S)-K_1(t,S_1)\| &\leqslant \left\{\frac{\partial K_1}{\partial S}\right\}\|S(t)-S_1(t)\| \quad (25)\\
&\leqslant \{\theta_1\}\|S(t)-S_1(t)\|
\end{aligned}$$

where θ_1 is defined in Eq. (22). Following the same for the remaining kernels will satisfy the following:

$$\begin{aligned}
\|K_2(t,E)-K_2(t,E_1)\| &\leqslant \{\theta_2\}\|E(t)-E_1(t)\|;\\
\|K_3(t,I)-K_3(t,I_1)\| &\leqslant \{\theta_3\}\|I(t)-I_1(t)\|;\\
\|K_4(t,A)-K_4(t,A_1)\| &\leqslant \{\theta_4\}\|A(t)-A_1(t)\|;\\
\left\|K_5\left(t,S_q\right)-K_5\left(t,S_{q1}\right)\right\| &\leqslant \{\theta_5\}\left\|S_q(t)-S_{q1}(t)\right\|;\\
\left\|K_6\left(t,E_q\right)-K_6\left(t,E_{q1}\right)\right\| &\leqslant \{\theta_6\}\left\|E_q(t)-E_{q1}(t)\right\|;\\
\|K_7(t,H)-K_7(t,H_1)\| &\leqslant \{\theta_7\}\|H(t)-H_1(t)\|;\\
\|K_8(t,R)-K_8(t,R_1)\| &\leqslant \{\theta_8\}\|R(t)-R_1(t)\|.
\end{aligned}$$

where θ_i are defined in Eq. (22). Then, the Lipschitz circumstances are satisfied by all kernels.

Furthermore, since $0 \leqslant U = \max\{\theta_i : i=1,2,\ldots,8\} < 1$ the kernels are contractions. From Eq. (25), we have

$$\begin{aligned}
S(t) &= S(0)+\Omega(\rho_1)K_1(t,S)+\omega(\rho_1)\int_0^t K_1(z,S)dz; \quad (26)\\
E(t) &= E(0)+\Omega(\rho_2)K_2(t,E)+\omega(\rho_2)\textstyle\int_0^t K_2(z,E)dz;\\
I(t) &= I(0)+\Omega(\rho_3)K_3(t,I)+\omega(\rho_3)\textstyle\int_0^t K_3(z,I)dz;\\
A(t) &= A(0)+\Omega(\rho_4)K_4(t,A)+\omega(\rho_4)\textstyle\int_0^t K_4(z,A)dz;\\
S_q(t) &= S_q(0)+\Omega(\rho_5)K_5\left(t,S_q\right)+\omega(\rho_5)\textstyle\int_0^t K_5\left(z,S_q\right)dz;\\
E_q(t) &= E_q(0)+\Omega(\rho_6)K_6\left(t,E_q\right)+\omega(\rho_6)\textstyle\int_0^t K_6\left(z,E_q\right)dz;\\
H(t) &= H(0)+\Omega(\rho_7)K_7(t,H)+\omega(\rho_7)\textstyle\int_0^t K_7(z,H)dz;\\
R(t) &= R(0)+\Omega(\rho_8)K_8(t,R)+\omega(\rho_8)\textstyle\int_0^t K_8(z,R)dz.
\end{aligned}$$

Utilizing Eq. (23), The next recursive relations are being produced now.

Please cite this article in press as: M. Higazy, M.A. Alyami, New Caputo-Fabrizio fractional order $SEIAS_qE_qHR$ model for COVID-19 epidemic transmission with genetic algorithm based control strategy, Alexandria Eng. J. (2020), https://doi.org/10.1016/j.aej.2020.08.034

$$S_n(t) = \Omega(\rho_1)K_1(t, S_{n-1}) + \omega(\rho_1)\int_0^t K_1(z, S_{n-1})dz; \quad (27)$$

$$E_n(t) = \Omega(\rho_2)K_2(t, E_{n-1}) + \omega(\rho_2)\int_0^t K_2(z, E_{n-1})dz;$$

$$I_n(t) = \Omega(\rho_3)K_3(t, I_{n-1}) + \omega(\rho_3)\int_0^t K_3(z, I_{n-1})dz;$$

$$A_n(t) = \Omega(\rho_4)K_4(t, A_{n-1}) + \omega(\rho_4)\int_0^t K_4(z, A_{n-1})dz;$$

$$S_{q,n}(t) = \Omega(\rho_5)K_5\left(t, S_{q,(n-1)}\right) + \omega(\rho_5)\int_0^t K_5\left(z, S_{q,(n-1)}\right)dz;$$

$$E_{q,n}(t) = \Omega(\rho_6)K_6\left(t, E_{q,n-1}\right) + \omega(\rho_6)\int_0^t K_6\left(z, E_{q,n-1}\right)dz;$$

$$H_n(t) = \Omega(\rho_7)K_7(t, H_{n-1}) + \omega(\rho_7)\int_0^t K_7(z, H_{n-1})dz;$$

$$R_n(t) = \Omega(\rho_8)K_8(t, R_{n-1}) + \omega(\rho_8)\int_0^t K_8(z, R_{n-1})dz.$$

where

$$S(0) = S_0(t); E(0) = E_0(t); I(0) = I_0(t); A(0) = A_0(t);$$
$$S_q(0) = S_{q,0}(t); E_q(0) = E_{q,0}(t); H(0) = H_0(t); R(0) = R_0(t).$$

The recursive relations for this system can be written as

$$\mathscr{S}_n(t) = \Omega(\rho_1)(K_1(t, S_{n-1}) - K_1(t, S_{n-2})) \quad (28)$$
$$+\omega(\rho_1)\int_0^t (K_1(z, S_{n-1}) - K_1(z, S_{n-2}))dz;$$
$$\mathscr{E}_n(t) = \Omega(\rho_2)(K_2(t, E_{n-1}) - K_2(t, E_{n-2}))$$
$$+\omega(\rho_2)\int_0^t (K_2(z, E_{n-1}) - K_2(z, E_{n-2}))dz;$$
$$\mathscr{I}_n(t) = \Omega(\rho_3)(K_3(t, I_{n-1}) - K_3(t, I_{n-2}))$$
$$+\omega(\rho_3)\int_0^t (K_3(z, I_{n-1}) - K_3(z, I_{n-2}))dz;$$
$$\mathscr{A}_n(t) = \Omega(\rho_4)(K_4(t, A_{n-1}) - K_4(t, A_{n-2}))$$
$$+\omega(\rho_4)\int_0^t (K_4(z, A_{n-1}) - K_4(z, A_{n-2}))dz;$$
$$\mathscr{S}_{q,n}(t) = \Omega(\rho_5)\left(K_5\left(t, S_{q,(n-1)}\right) - K_5\left(t, S_{q,(n-2)}\right)\right)$$
$$+\omega(\rho_5)\int_0^t \left(K_5\left(z, S_{q,(n-1)}\right) - K_5\left(z, S_{q,(n-2)}\right)\right)dz;$$
$$\mathscr{E}_q(t) = \Omega(\rho_6)\left(K_6\left(t, E_{q,n-1}\right) - K_6\left(t, E_{q,n-2}\right)\right)$$
$$+\omega(\rho_6)\int_0^t \left(K_6\left(z, E_{q,n-1}\right) - K_6\left(z, E_{q,n-2}\right)dz;\right.$$
$$\mathscr{H}_n(t) = \Omega(\rho_7)(K_7(t, H_{n-1}) - K_7(t, H_{n-2}))$$
$$+\omega(\rho_7)\int_0^t (K_7(z, H_{n-1}) - K_7(z, H_{n-2})dz;$$
$$\mathscr{R}_n(t) = \Omega(\rho_8)(K_8(t, R_{n-1}) - K_8(t, R_{n-2}))$$
$$+\omega(\rho_8)\int_0^t (K_8(z, R_{n-1}) - K_8(z, R_{n-2}))dz.$$

$$S_n(t) = \sum_{i=1}^{n}\mathscr{S}_i(t);\ E_n(t) = \sum_{i=1}^{n}\mathscr{E}_i(t);$$
$$I_n(t) = \sum_{i=1}^{n}\mathscr{I}_i(t);\ S_{q,n}(t) = \sum_{i=1}^{n}\mathscr{S}_{q,i}(t); \quad (29)$$
$$E_{q,n}(t) = \sum_{i=1}^{n}\mathscr{E}_{q,i}(t);\ A_n(t) = \sum_{i=1}^{n}\mathscr{A}_i(t);$$
$$H_n(t) = \sum_{i=1}^{n}\mathscr{H}_i(t);\ R_n(t) = \sum_{i=1}^{n}\mathscr{R}_i(t).$$

And

$$\|\mathscr{S}_n(t)\| = \|S_n - S_{n-1}\| = \quad (30)$$
$$\Big\|\Omega(\rho_1)(K_1(t, S_{n-1}) - K_1(t, S_{n-2})) + \omega(\rho_1)\int_0^t (K_1(z, S_{n-1})$$
$$- K_1(z, S_{n-2}))dz\Big\|$$

By applying Eq. (30) in triangle inequality, we get

$$\|S_n - S_{n-1}\| \leqslant \Omega(\rho_1)\|(K_1(t, S_{n-1}) - K_1(t, S_{n-2}))\| \quad (31)$$
$$+ \omega(\rho_1)\int_0^t \|(K_1(z, S_{n-1}) - K_1(z, S_{n-2}))dz\|$$

So, because the kernel K_1 satisfies the Lipschitz condition with Lipschitz constant θ_1, then we have

$$\|S_n - S_{n-1}\| \leqslant \Omega(\rho_1)\theta_1\|S_{n-1} - S_{n-2}\| + \omega(\rho_1)$$
$$\times \int_0^t \|S_{n-1}(z) - S_{n-2}(z)\|dz \quad (32)$$

Then we have

$$\|\mathscr{S}_n\| \leqslant \Omega(\rho_1)\theta_1\|\mathscr{S}_{n-1}\| + \omega(\rho_1)\int_0^t \|\mathscr{S}_{n-1}(z)\|dz \quad (33)$$

The following can be obtained by the similar reasoning

$$\|\mathscr{E}_n\| \leqslant \Omega(\rho_2)\theta_2\|\mathscr{E}_{n-1}\| + \omega(\rho_2)\int_0^t \|\mathscr{E}_{n-1}(z)\|dz \quad (34)$$

$$\|\mathscr{I}_n\| \leqslant \Omega(\rho_3)\theta_3\|\mathscr{I}_{n-1}\| + \omega(\rho_3)\int_0^t \|\mathscr{I}_{n-1}(z)\|dz \quad (35)$$

$$\|\mathscr{A}_n\| \leqslant \Omega(\rho_4)\theta_4\|\mathscr{A}_{n-1}\| + \omega(\rho_4)\int_0^t \|\mathscr{A}_{n-1}(z)\|dz \quad (36)$$

$$\left\|\mathscr{S}_{q,n}\right\| \leqslant \Omega(\rho_5)\theta_5\left\|\mathscr{S}_{q,n-1}\right\| + \omega(\rho_5)\int_0^t \left\|\mathscr{S}_{q,n-1}(z)\right\|dz \quad (37)$$

$$\left\|\mathscr{E}_{q,n}\right\| \leqslant \Omega(\rho_6)\theta_6\left\|\mathscr{E}_{q,n-1}\right\| + \omega(\rho_6)\int_0^t \left\|\mathscr{E}_{q,n-1}(z)\right\|dz \quad (38)$$

$$\|\mathscr{H}_n\| \leqslant \Omega(\rho_7)\theta_7\|\mathscr{H}_{n-1}\| + \omega(\rho_7)\int_0^t \|\mathscr{H}_{n-1}(z)\|dz \quad (39)$$

$$\|\mathscr{R}_n\| \leqslant \Omega(\rho_8)\theta_8\|\mathscr{R}_{n-1}\| + \omega(\rho_8)\int_0^t \|\mathscr{R}_{n-1}(z)\|dz \quad \square \quad (40)$$

Theorem 3.4. *Let there is $t_0 > 0$ such that $\Omega(\rho_j)\theta_j + \omega(\rho_j)\theta_j t_0 < 1$ where $j = 1, 2, \ldots, 8$. Then the solution of the proposed paradigm (2) exists.*

Proof. Because all of the functions, $S(t)$, $E(t)$, $I(t)$, $A(t)$, $S_q(t)$, $E_q(t)$, $H(t)$ and $R(t)$, are bounded and all of the kernels meet a Lipschitz condition, the existence and smoothness of the solutions in (29) are proved. For the proof to be finished, the convergence of $S(t)$, $E(t)$, $I(t)$, $A(t)$, $S_q(t)$, $E_q(t)$, $H(t)$ and $R(t)$, the solutions of (2), are going to be proved here. Define $S_n^*(t)$, $E_n^*(t)$, $I_n^*(t)$, $A_n^*(t)$, $S_{q,n}^*(t)$, $E_{q,n}^*(t)$, $H_n^*(t)$ and $R_n^*(t)$ such that

$$S(t)-S(0)=S_n(t)-S_n^*(t);E(t)-E(0)=E_n(t)-E_n^*(t); \quad (41)$$

$$I(t)-I(0) \quad =I_n(t)-I_n^*(t);A(t)-A(0)=A_n(t)-A_n^*(t);$$

$$S_q(t)-S_q(0)=S_{q,n}(t)-S_{q,n}^*(t);E_q(t)-E_q(0)=E_{q,n}(t)-E_{q,n}^*(t);$$

$$H(t)-H(0)=H_n(t)-H_n^*(t);R(t)-R(0)=R_n(t)-R_n^*(t);$$

For K_1 we get

$$\begin{aligned}\left\|S_n^*(t)\right\| &= \Big\|\Omega(\rho_1)(K_1(t,S)-K_1(t,S_{n-1})) \\ &\quad +\omega(\rho_1)\int_0^t (K_1(z,S)-K_1(z,S_{n-1}))dz\Big\| \quad (42)\\ &\leqslant \Omega(\rho_1)\|K_1(t,S)-K_1(t,S_{n-1})\|+\omega(\rho_1)\textstyle\int_0^t \|K_1(z,S) \\ &\quad -K_1(z,S_{n-1})\|dz \\ &\leqslant \Omega(\rho_1)\theta_1\|S-S_{n-1}\|+\omega(\rho_1)\theta_1\|S-S_{n-1}\|dz\end{aligned}$$

Recursively, repeat the above steps, we obtain

$$\left\|S_n^*(t)\right\| \leqslant [\Omega(\rho_1)\theta_1+\omega(\rho_1)\theta_1 t]^{n+1}\gamma_1 \quad (43)$$

So at t_0, we have

$$\left\|S_n^*(t)\right\| \leqslant [\Omega(\rho_1)\theta_1+\omega(\rho_1)\theta_1 t_0]^{n+1}\gamma_1 \quad (44)$$

Via taking the limit on Eq. (44) while $n\to\infty$, we get $\left\|S_n^*(t)\right\|\to 0$. Similarly, we get $\left\|E_n^*(t)\right\|\to 0$, $\left\|I_n^*(t)\right\|\to 0$, $\left\|A_n^*(t)\right\|\to 0$, $\left|S_{q,n}^*(t)\right|\to 0$, $\left|E_{q,n}^*(t)\right|\to 0$, $\left\|H_n^*(t)\right\|\to 0$ and $\left\|R_n^*(t)\right\|\to 0$. The existence of system solutions is hence proved. □

Theorem 3.5. *The fraction order ($SEIAS_qE_qHR$)-model (2), with the initial conditions (3), has a unique solution if the next conditions are met:*

$$(1-\Omega(\rho_i)-\omega(\rho_i))\theta_i t>0 \quad (45)$$

for $i=1,2,\ldots,8$.

Proof. Suppose that $S_1(t)$, $E_1(t)$, $I_1(t)$, $A_1(t)$, $S_{q,1}(t)$, $E_{q,1}(t)$, $H_1(t)$ and $R_1(t)$ for the current solution in the previous theorem, so we have

$$\begin{aligned}S(t)-S_1(t) &= \Omega(\rho_1)(K_1(t,S)-K_1(t,S_1)) \quad (46)\\ &\quad +\omega(\rho_1)\textstyle\int_0^t (K_1(z,S)-K_1(t,S_1))dz \\ \|S(t)-S_1(t)\| &\leqslant \Omega(\rho_1)\|K_1(t,S)-K_1(t,S_{n-1})\| \\ &\quad +\omega(\rho_1)\textstyle\int_0^t \|K_1(z,S)-K_1(z,S_{n-1})\|dz\end{aligned}$$

Then

$$\begin{aligned}\|S(t)-S_1(t)\| &\leqslant \Omega(\rho_1)\theta_1\|S-S_1\| \\ &\quad +\omega(\rho_1)\theta_1 t\|S-S_{n-1}\| \quad (47)\end{aligned}$$

Reorder (47)

$$\|S(t)-S_1(t)\|(1-\Omega(\rho_1)\theta_1-\omega(\rho_1)\theta_1 t)\leqslant 0 \quad (48)$$

Combine the condition in (45) for $i=1$ with Eq. (48), we get

$$\|S(t)-S_1(t)\|=0$$

and then $S(t)=S_1(t)$. Also, It is true for $E_1(t)$, $I_1(t)$, $A_1(t)$, $S_{q,1}(t)$, $E_{q,1}(t)$, $H_1(t)$ and $R_1(t)$. Consequently, the uniqueness of the solution scheme for the fractional derivative order system is proved. □

4. Numerical simulations and results discussion

The non-linear system of the fractional order differential equations of COVID-19 ($SEIAS_qE_qHR$)-model has been modeled by utilizing the Caputo fraction derivative. The impacts of the system parameters on the dynamics of the fractional-order model (2), can be done via (2) numerically using the parameters' values recorded in Table 1 with finite time. The numerical integrations needed for the fractional order COVID-19 ($SEIAS_qE_qHR$)-model are executed in this paper via the predictor-corrector Adams-Bashforth-Moulton (ABM) technique for fractional order differential equations, constructed by Diethelm et al. [57]. These simulations detect that changing the values of the fractional order, contact rate or quarantine rate affects the dynamics of the model.

Fig. 2 shows the time history of COVID-19 fractional order ($SEIAS_qE_qHR$)-model according to various fractional derivative orders $\rho=0.7,\ 0.8,\ 0.9,\ 1$; (a) Susceptible humans $S(t)$ versus time in days, (b) Exposed humans $E(t)$ versus time in days, (c) Infected with symptoms humans $I(t)$, (d) Infected humans without symptoms versus time in days. The arrows directions indicate the effect of increasing the fractional order ρ. Fig. 3 shows the time history of COVID-19 ($SEIAS_qE_qHR$)-model according to various fractional derivative orders $\rho=0.7,\ 0.8,\ 0.9,\ 1$; (a) Quarantined Susceptible humans $S_q(t)$ versus time in days, (b) Quarantined exposed humans $E_q(t)$ versus time in days, (c) Hospitalised humans $H(t)$ versus time in days, (d) Recuperated humans without symptoms versus time in days. The arrows directions indicate the effect of increasing the fractional order ρ. Fig. 4 shows the impact of changing the contact rate c on the dynamics of all population classes at fractional order $\rho=1$. The arrow direction indicates increasing the contact rate where the estimated basic contact rate $c=14.781$. From Figs. 2–4, decreasing the fractional derivative order delays the peak values and makes the curves more flat.

Table 1 Parameter values estimated for fractional order COVID-19 ($SEIAS_qE_qHR$)-model.

Parameter	Estimated value c.f. [21]
c	14.781
β	$2.1011/10^8$
q	$1.8887/10^7$
σ	1/7
λ	1/14
l	0.86834
δ_I	0.13266
δ_q	0.1259
γ_I	0.33029
γ_A	0.13978
γ_H	0.11624
θ	0.8
α	$1.782610/10^5$

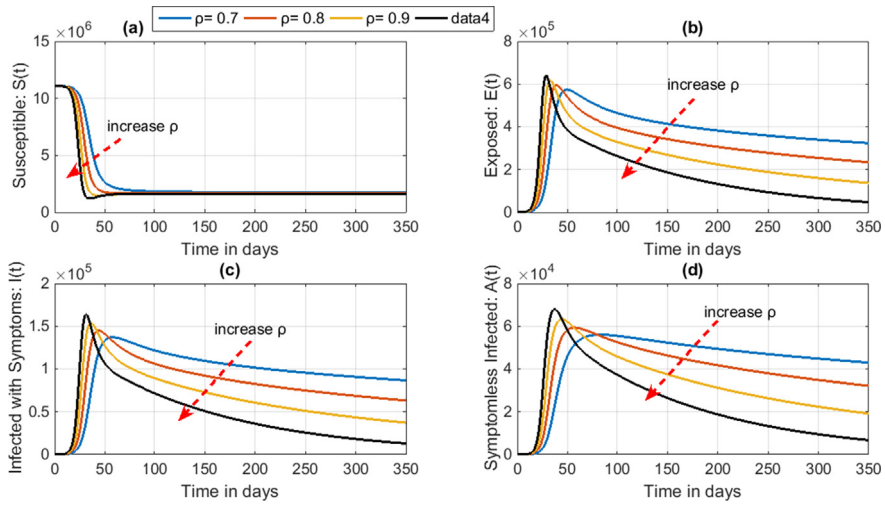

Fig. 2 The time history of COVID-19 ($SEIAS_qE_qHR$)-model according to different fractional derivative order $\rho = 0.7,\ 0.8,\ 0.9,\ 1$; (a) Susceptible humans $S(t)$ versus time in days, (b) Exposed humans $E(t)$ versus time in days, (c) Infected with symptoms humans $I(t)$, (d) Infected humans without symptoms versus time in days. The directions of arrows indicate the effect of increasing the fractional order ρ.

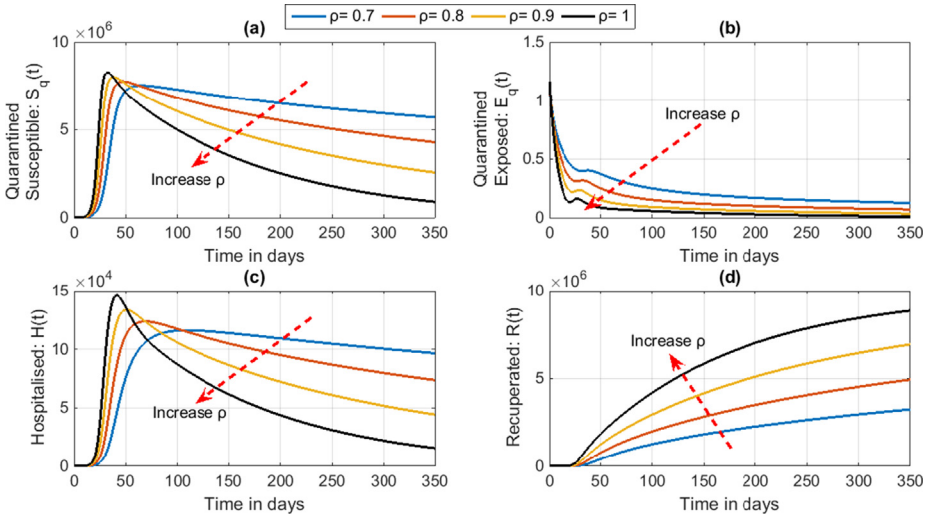

Fig. 3 The time history of COVID-19 ($SEIAS_qE_qHR$)-model according to different fractional derivative order $\rho = 0.7,\ 0.8,\ 0.9,\ 1$; (a) Quarantined Susceptible humans $S_q(t)$ versus time in days, (b) Quarantined exposed humans $E_q(t)$ versus time in days, (c) Hospitalised humans $H(t)$ versus time in days, (d) Recuperated humans without symptoms versus time in days. The directions of arrows indicate the effect of increasing the fractional order ρ.

Fig. 5 shows the impact of changing the contact rate c on the dynamics of all population classes at fractional order $\rho = 0.9$. The direction of the arrow indicates increasing the contact rate where the estimated basic contact rate $c = 14.781$. Fig. 6 shows the impact of changing the contact rate c on the dynamics of all population classes at fractional order $\rho = 0.8$. The direction of the arrow indicates increasing the contact rate where the estimated basic contact rate $c = 14.781$. Fig. 7 shows the impact of changing both contact rate and fractional order on all population classes at day 40. From which we can say that the contact rate has a great impact on the system dynamics of the system and has a great impact on the total number of infected classes.

Fig. 8 shows the impact of changing the quarantining rate q on the dynamics of all population classes at fractional order $\rho = 0.8$. The direction of the arrow indicates increasing the quarantining rate where the estimated basic contact rate $q = 1.8887 * 10\hat{}7$. Fig. 9 shows the impact of changing the quarantining rate q on the dynamics of all population classes at fractional order $\rho = 0.9$. The direction of the arrow indicates increasing the quarantining rate where the estimated basic contact rate $q = 1.8887 * 10\hat{}7$. Fig. 10 shows the impact of changing the quarantining rate q on the dynamics of all population classes at fractional order $\rho = 1$. The arrow direction indicates increasing the quarantining rate where the estimated basic contact rate $q = 1.8887 * 10\hat{}7$. Fig. 11 shows the impact of changing both quarantining rate and fractional order on all population classes at day 40. From which we can deduce that quarantining has a great impact on the total number of infected classes.

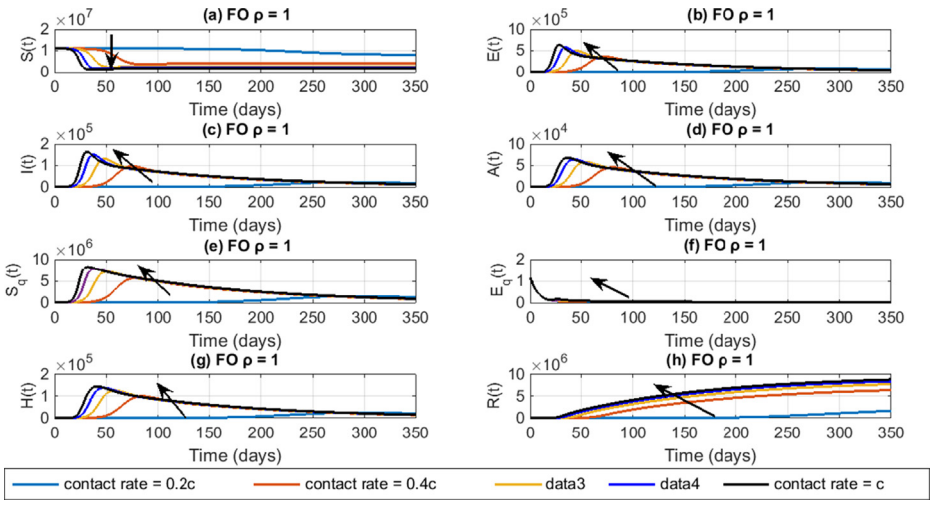

Fig. 4 The impact of changing the contact rate c on the dynamics of all population classes at fractional order $\rho = 1$. The direction of the arrow indicates increasing the contact rate where the estimated basic contact rate $c = 14.781$.

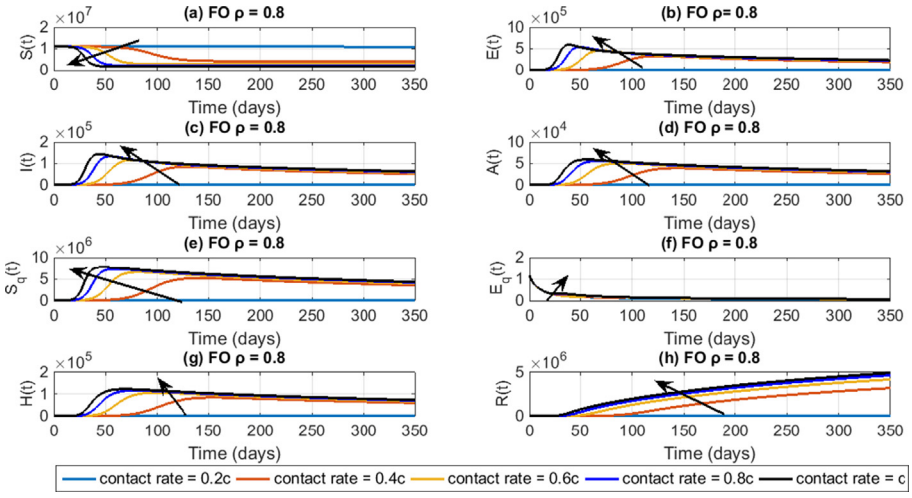

Fig. 5 The impact of changing the contact rate c on the dynamics of all population classes at fractional order $\rho = 0.9$. The direction of the arrow indicates increasing the contact rate where the estimated basic contact rate $c = 14.781$.

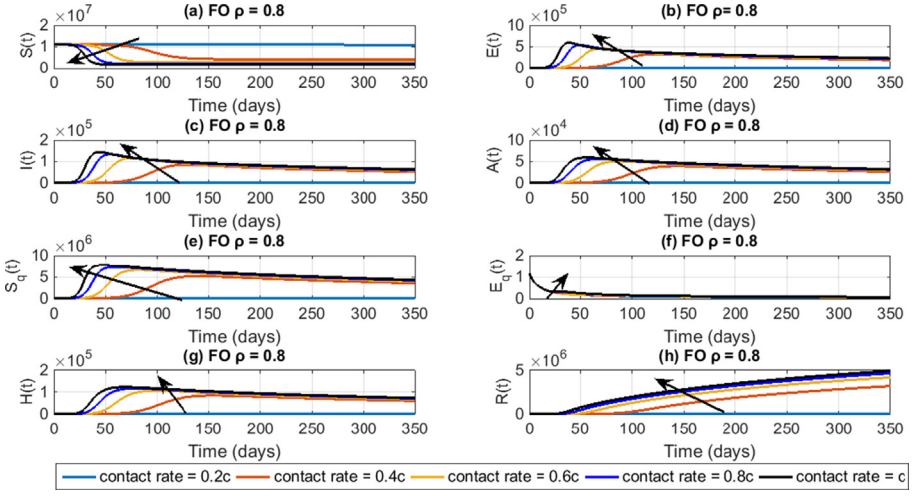

Fig. 6 The impact of changing the contact rate c on the dynamics of all population classes at fractional order $\rho = 0.8$. The direction of the arrow indicates increasing the contact rate where the estimated basic contact rate $c = 14.781$.

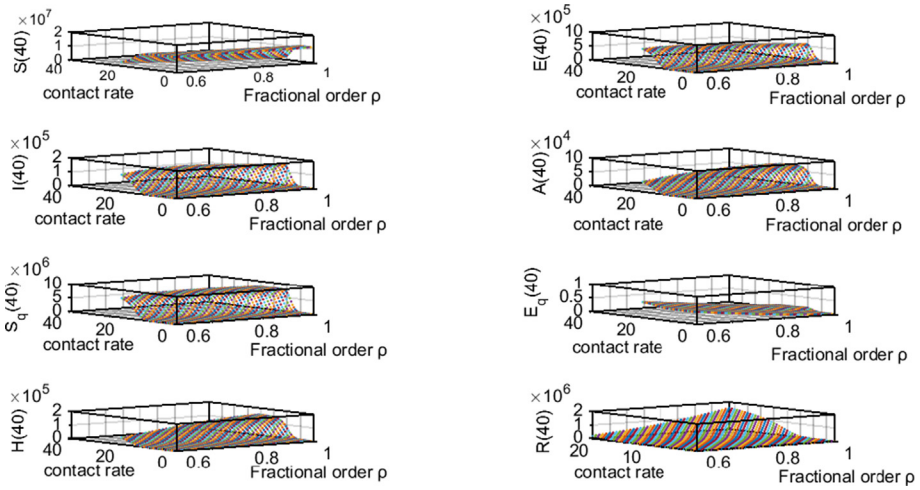

Fig. 7 Impact of changing both contact rate and fractional order on all population classes at day 40.

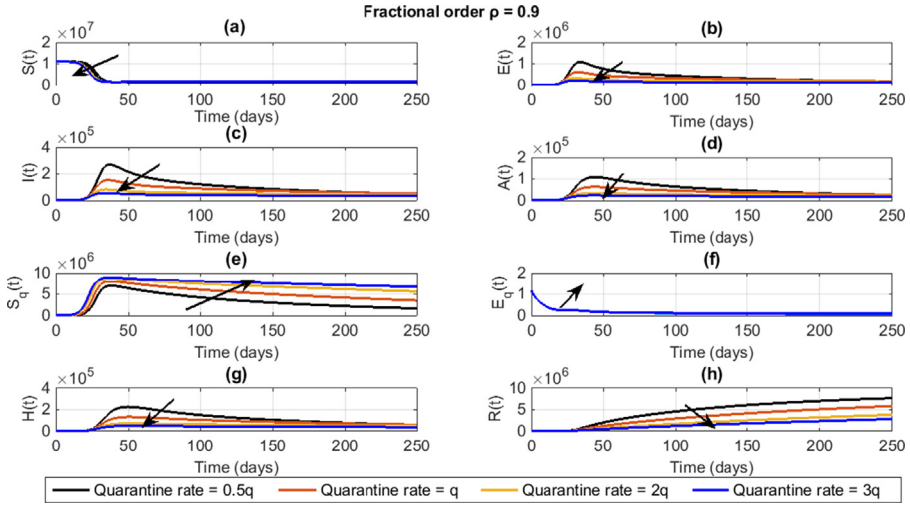

Fig. 8 The impact of changing the quarantining rate q on the dynamics of all population classes at fractional order $\rho = 0.8$. The direction of the arrow indicates increasing the quarantine rate where the estimated basic contact rate $q = 1.8887 * 10\hat{}7$.

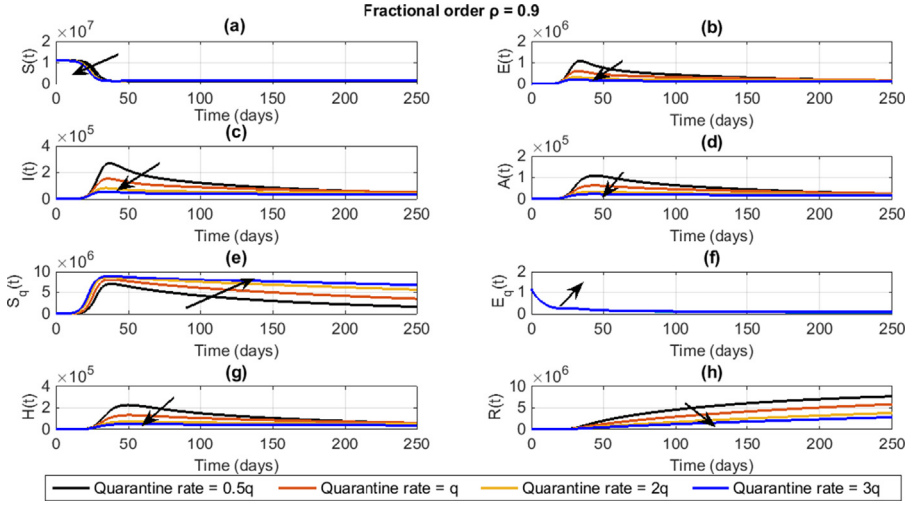

Fig. 9 The impact of changing the quarantining rate q on the dynamics of all population classes at fractional order $\rho = 0.9$. The direction of the arrow indicates increasing the quarantine rate where the estimated basic contact rate $q = 1.8887 * 10\hat{}7$.

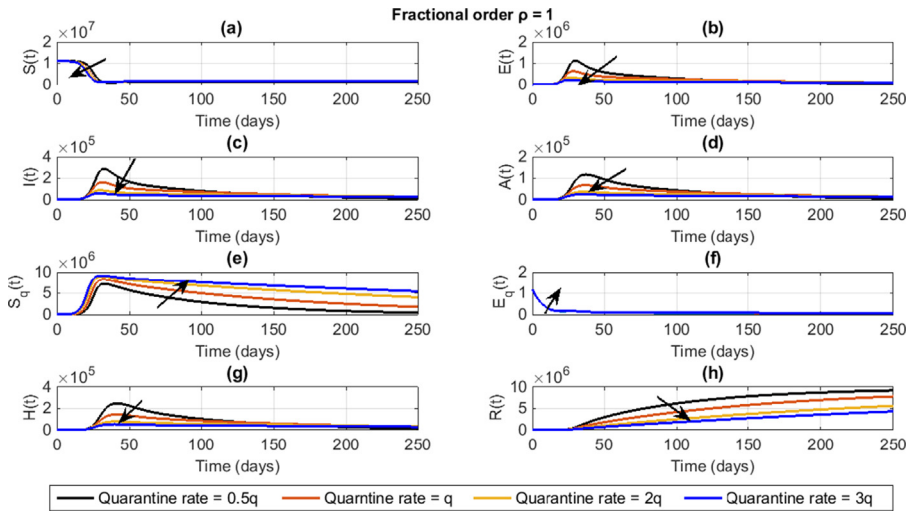

Fig. 10 The impact of changing the quarantining rate q on the dynamics of all population classes at fractional order $\rho = 1$. The direction of the arrow indicates increasing the quarantine rate where the estimated basic contact rate $q = 1.8887 * 10\hat{}7$.

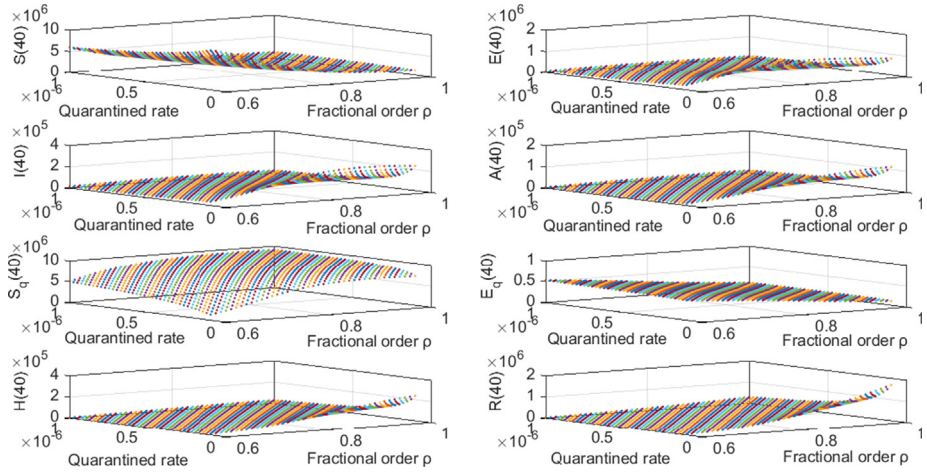

Fig. 11 Impact of changing both quarantining rate and fractional order on all population classes at day 40.

5. Genetic algorithm based control strategy

In the current section, we numerically study different control strategies for the proposed COVID-19 fractional order ($SEIAS_qE_qHR$)-model utilizing the contact rate, c, and quarantining rate, q, parameters. The logistic requirements may limit the minimum contact rate and the maximum quarantining rate. So, our optimum control problem is to search for the optimum values of the two control parameters that minimizes the peak values of the two infected classes within these limitations.

Fig. 12 shows the effect of changing the two control parameters on the different classes of COVID-19 fractional order ($SEIAS_qE_qHR$)-model at day 40 with fractional derivative order $\rho = 0.95$. Using the genetic algorithm toolbox of MATLAB [44], the optimum values of the two control parameters that minimizes the sum of peak values of the two infected classes.

Let the system population classes vector be $X = \left(S, E, I, A, S_q, E_q, H, R\right)^{tr}$. The under control reproduction number calculated in [21], following [58], is

$$R_c = \left[\frac{\beta lc - \beta lcq}{\delta_I + \alpha + \gamma_I} + \frac{\beta cc\theta(1-q)(1-l)}{\gamma_A}\right] S_0$$

The control problem is to choose the optimum values of the two control parameters c and q in order to minimize the proposed fitness function $(\sum(I) + \sum(A))$as:

$$Min\left(\sum(I) + \sum(A)\right) \tag{49}$$

s.t.

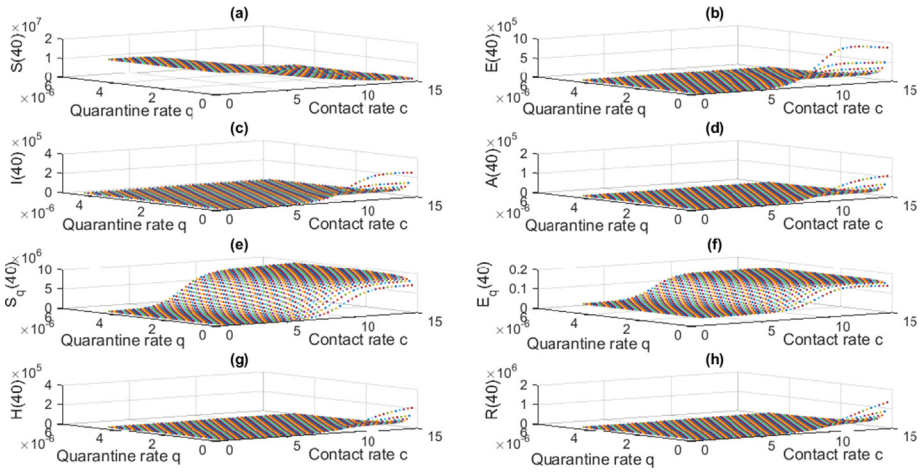

Fig. 12 Impact of changing both contact rate and quarantining rate on all population classes at day 40 with fractional derivative order $\rho = 0.95$.

$$1.5 < R_c < R_{c\max},\ c_{\min} \leqslant c \leqslant c_{\max},\ q_{\min} \leqslant c \leqslant q_{\max}, \tag{50}$$

$$\begin{aligned}
{}^{CF}\Delta_t^{\rho_1} S(t) = {} & -(\beta c + cq(1-\beta))S(t)I(t) \\
& -(\beta c + cq(1-\beta))\theta S(t)A(t) + \lambda S_q(t); \\
{}^{CF}\Delta_t^{\rho_2} E(t) = {} & \beta c(1-q)S(t)I(t) + \beta c(1-q)\theta S(t)A(t) - \sigma E(t); \\
{}^{CF}\Delta_t^{\rho_3} I(t) = {} & \sigma l E(t) - (\delta_I + \alpha + \gamma_I)I(t); \\
{}^{CF}\Delta_t^{\rho_4} A(t) = {} & \sigma(1-l)E(t) - \gamma_A A(t); \\
{}^{CF}\Delta_t^{\rho_5} S_q(t) = {} & cq(1-\beta)S(t)I(t) + cq\theta(1-\beta)S(t)A(t) - \lambda S_q(t); \\
{}^{CF}\Delta_t^{\rho_6} E_q(t) = {} & \beta cqS(t)I(t) + \beta cq\theta S(t)A(t) - \delta_q E_q(t); \\
{}^{CF}\Delta_t^{\rho_7} H(t) = {} & \delta_I I(t) + \delta_q E_q(t) - (\alpha + \gamma_H)H(t); \\
{}^{CF}\Delta_t^{\rho_8} R(t) = {} & \gamma_I I(t) + \gamma_A A(t) + \gamma_H H(t).
\end{aligned}$$

Case 5.1. Using the genetic algorithm via MATLAB optimization toolbox, the optimum values of the contact rate is found as $c^* = 3.4179$ and quarantine rate $q^* = 4.707 \times 10^{-6}$ which equal the $q_{\max}$ (25 times the quarantine rate that is estimated from the real data in [21]), where $R_{c\max} = 6.5$, $R_{c\min} = 1.5$, $c_{\min} = 1.5$, $c_{\max} = 15$, $q_{\min} = 1.8887 \times 10^{-7}$, $q_{\max} = 25 * q_{\min}$ and the other system parameters and the initial values are as in the previous section. The minimum fitness value (sum of infected cases (49)) is about 1657 cases.

Case 5.2. Using the genetic algorithm via MATLAB optimization toolbox, the optimum values of the contact rate is found as $c^* = 2.2787$ and quarantine rate $q^* = 4.72175 \times 10^{-6}$ which equal the $q_{\max}$ (25 times the quarantine rate that is estimated from the real data in [21]), where $R_{c\max} = 6.5$, $R_{c\min} = 1$, $c_{\min} = 2$, $c_{\max} = 15$, $q_{\min} = 1.8887 \times 10^{-7}$, $q_{\max} = 25 * q_{\min}$, and the other system parameters and the initial values are as in the previous section. The minimum fitness value (sum of infected cases (49)) is about 4626 cases.

Case 5.3. Let the fitness function be

$$\left(\sum(E) + \sum(I) + \sum(A) + \sum(S_q) + \sum(E_q) + \sum(H)\right)$$

Using the genetic algorithm via MATLAB optimization toolbox, the optimum values of the contact rate is found as $c^* = 2.2787$ and quarantine rate $q^* = 4.72175 \times 10^{-6}$ which equal the $q_{\max}$ (25 times the quarantine rate that is estimated from the real data in [21]), where $R_{c\max} = 6.5$, $R_{c\min} = 1$, $c_{\min} = 2$, $c_{\max} = 15$, $q_{\min} = 1.8887 \times 10^{-7}$, $q_{\max} = 25 * q_{\min}$, and the other system parameters and the initial values are as in the previous section. The minimum fitness value is 23,617 cases.

Fig. 13 displays the optimization process by genetic algorithm Case 5.1. Fig. 14 displays the optimization process by genetic algorithm Case 5.2. Fig. 15 displays the optimization process by genetic algorithm Case 5.3. Fig. 16 shows the effect of the two control parameters c and q on the controlled reproduction number R_c. From Fig. 16, we see that the contact rate has a great impact on the reproduction number but the quarantine rate has a low impact on the reproduction number. The reproduction number at the optimum values of the two control parameters is $R_c(c^*, q^*) = 1.5$, which equal the minimum possible reproduction number in our proposed optimization case.

Fig. 17 shows the dynamics of COVID-19 fractional order ($SEIAS_qE_qHR$)-model with different fractional order $\rho = 0.8,\ 0.9$ and 1. The directions of the arrows in Fig. 17 indicate the direction of increasing the fractional derivative order. From Fig. 18, the number of individuals in the two infected classes are clearly minimized and the minimum of the sum of the infected classes is 1657.28 only. Fig. 18 shows the dynamics of COVID-19 fractional order ($SEIAS_qE_qHR$)-model with different fractional order $\rho = 0.8,\ 0.9$ and 1. The directions of the arrows in Fig. 18 indicate the direction of increasing the fractional derivative order. From Fig. 18, the number of individuals in the two infected classes are clearly minimized and the minimum of the sum of the infected classes is 4626 cases.

6. Conclusion

We have studied theoretically and numerically a fractional order model for COVID-19 transmission under genetic algorithm based control strategies. The integer order $SEIAS_qE_qHR$ model proposed by Biao Tang et al. (2020)

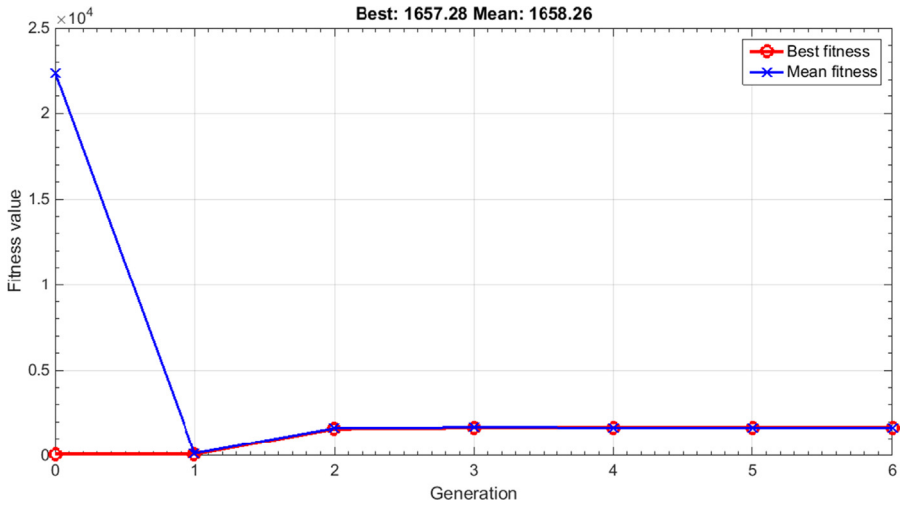

Fig. 13 Optimisation process by genetic algorithm Case 1.

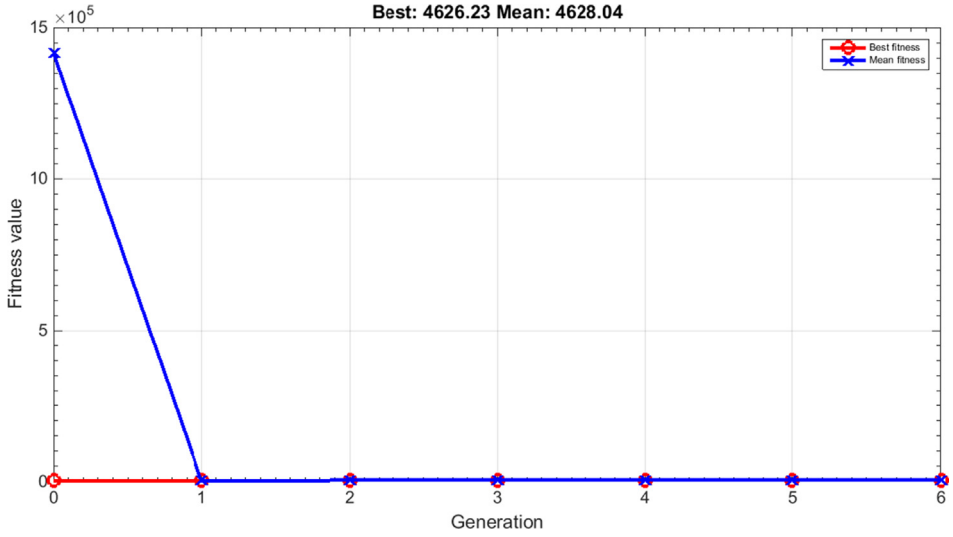

Fig. 14 Optimisation process by genetic algorithm Case 2.

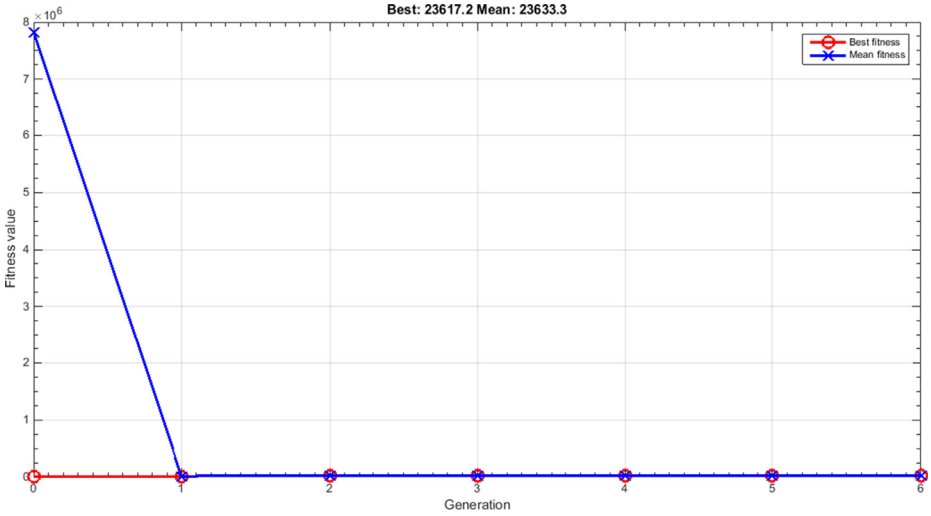

Fig. 15 Optimisation process by genetic algorithm Case 3.

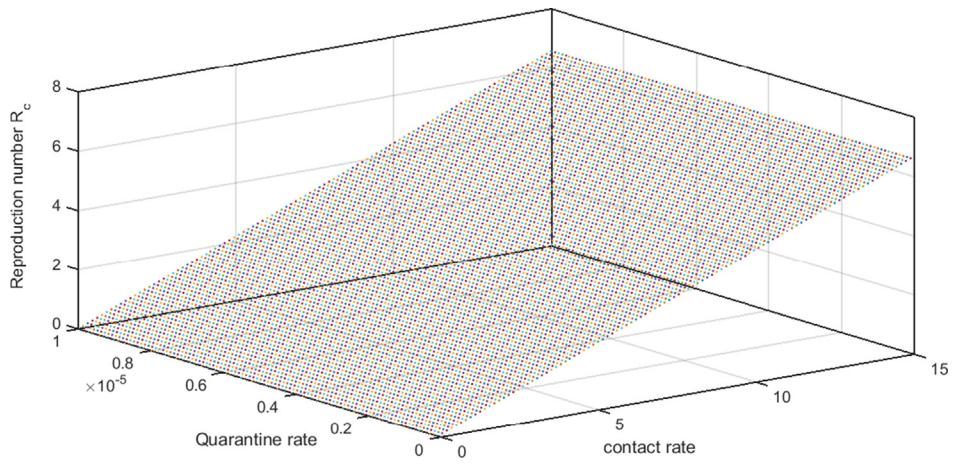

Fig. 16 The controlled reproduction number R_c sensitivity with respect to both contact rate c and quarantining rate q.

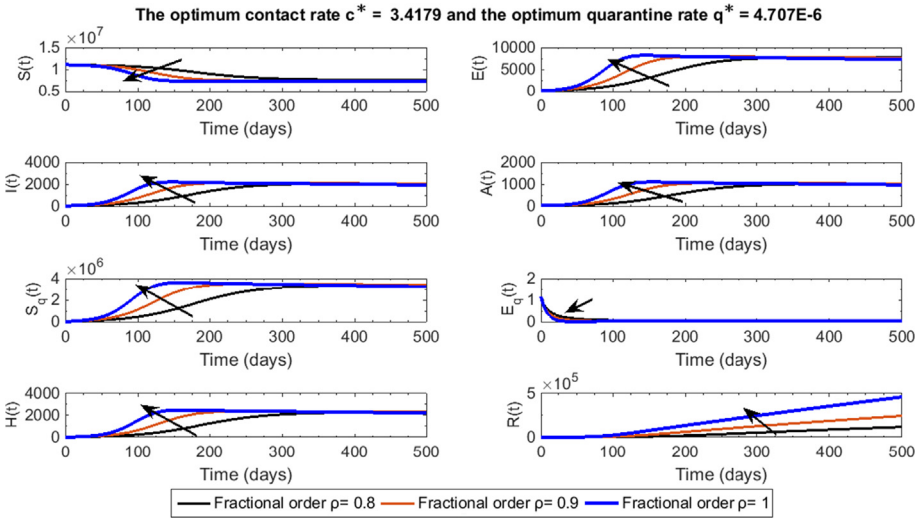

Fig. 17 The dynamics of COVID-19 fractional order ($SEIAS_qE_qHR$)-model with optimum contact rate $c^* = 3.179$ and optimum quarantine rate $q^* = 4.707E-6$ which computed by genetic algorithm (Case 1). The directions of the arrows indicate the effect of increasing the fractional order.

in [21] has been generalized here to become a fractional order model via Caputo-Fabrizio fractional order differential operator. The stability of the proposed generalized COVID-19 fractional order $SEIAS_qE_qHR$ model has been discussed. The existence and uniqueness of solution of Caputo-Fabrizio fractional derivative order ($SEIAS_qE_qHR$) model have been investigated and proved. The impact of changing the fractional derivative order ρ, contact rate parameter c and quarantining rate parameter q have been displayed numerically. Utilizing genetic algorithm MATLAB optimization toolbox, three control cases have been investigated. From inspection of the numerical solution graphs, we can conclude the following:

- as the fractional derivative order ρ is decreased there is a related decrease in the number of infectious cases, and the peak values of the infected classes are decreased and delayed.
- the number of cases in the infected classes is strongly dependent on the contact rate, as the contact rate c is decreased the number of infected cases is decreased.
- the number of cases in the infected classes is weakly dependent on the quarantining rate, as the contact rate q is decreased the number of infected cases decreases.
- from GA optimization results, we recommend to take decisions to minimize the contact rate to its possible minimum value and to maximize the quarantining rate to its possible maximum value.

These results are in agreement with those obtained by Biao Tang et al. (2020) for $\rho = 1$ and suggest that the proposed fractional model is epidemiologically well-posed and is a proper elect.

For future work, we suggest to use the genetic algorithm to estimate the optimum values of the fractional derivative orders that minimize the errors between the real recorded data and

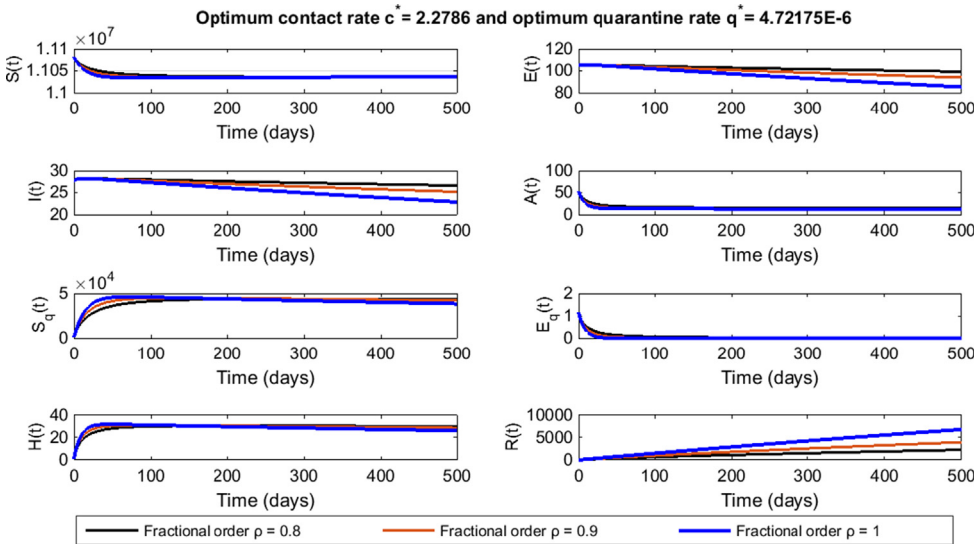

Fig. 18 The dynamics of COVID-19 fractional order ($SEIAS_qE_qHR$)-model with optimum contact rate $c^* = 2.2787$ and optimum quarantine rate $q^* = 4.72175E-6$ which computed by genetic algorithm (Case 2, Case 3). The directions of the arrows indicate the effect of increasing the fractional order.

the model solutions. In addition, we suggest to study the graph of the system via the graph theory concepts to discover more features of the model.

Funding

This research did not receive any specific grant from funding agencies in the public, commercial, or not-for-profit sectors.

Availaability of data and materials

Data sharing is not applicable to this paper as no datasets were generated or analyzed during the current study.

Declaration of Competing Interest

The authors declare that they have no known competing financial interests or personal relationships that could have appeared to influence the work reported in this paper.

References

[1] D.S.C. Hui, A. Zumla, Severe acute respiratory syndrome: Historical, epidemiologic, and clinical features, Infect. Dis. Clin. North Am. 33 (2019) 869–889.
[2] E. de Wit, N. van Doremalen, D. Falzarano, V.J. Munster, SARS and MERS: recent insights into emerging coronaviruses, Nat. Rev. Microbiol. 14 (2016) 523–534.
[3] M.E. Killerby, H.M. Biggs, C.M. Midgley, S.I. Gerber, J.T. Watson, Middle East respiratory syndrome coronavirus transmission, Emerg. Infect. Dis. 26 (2020) 191–198.
[4] K.H. Kim, T.E. Tandi, J.W. Choi, J.M. Moon, M.S. Kim, Middle East respiratory syndrome coronavirus (MERS-CoV) outbreak in South Korea, 2015: Epidemiology, characteristics and public health implications, J. Hosp. Infect. 95 (2017) 207–213.
[5] M. Willman, D. Kobasa, J. Kindrachuk, A Comparative analysis of factors influencing two outbreaks of middle eastern respiratory syndrome (MERS) in Saudi Arabia and South Korea, Viruses 11 (2019) 1119.
[6] K.O. Kwok, A. Tang, V.W.I. Wei, W.H. Park, E.K. Yeoh, S. Riley, Epidemic models of contact tracing: systematic review of transmission studies of severe acute respiratory syndrome and Middle East respiratory syndrome, Comput. Struct. Biotechnol. J. 17 (2019) 186–194.
[7] M. Egger, L. Johnson, C. Althaus, A. Schöni, G. Salanti, N. Low, S.L. Norris, Developing WHO guidelines: time to formally include evidence from mathematical modelling studies, F1000Research 6 (2017) 1584.
[8] T. Chen, J. Rui, Q. Wang, Z. Zhao, J.A Cui, L. Yin, A mathematical model for simulating the transmission of Wuhan novel coronavirus. bioRxiv 2020.
[9] N. Imai, I. Dorigatti, A. Cori, C. Donnelly, S. Riley, N.M. Ferguson, Report 2: Estimating the Potential Total Number of Novel Coronavirus Cases in Wuhan City, China. Available online: https://www.imperial.ac.uk/media/imperial-college/medicine/sph/ide/gida-fellowships/2019-nCoVoutbreak-report-22-01-2020.pdf (accessed on 23 January 2020).
[10] M.A. Khan, A. Atangana, Modeling the dynamics of novel coronavirus (2019-nCov) with fractional derivative, Alexandria Eng. J. (2020) –11. https://doi.org/10.1016/j.aej.2020.02.033.
[11] K.M. Owolabi, A. Atangana, Numerical Methods for Fractional Differentiation, Springer, Singapore, 2019.
[12] M.A. Khan, S. Ullah, M. Farooq, A new fractional model for tuberculosis with relapse via Atangana-Baleanu derivative, Chaos, Solit. Fract. 116 (2018) 227–238.
[13] E.O. Alzahrani, M.A. Khan, Modeling the dynamics of hepatitis E with optimal control, Chaos Solit. Fract. 116 (2018) 287–301.
[14] W. Gao, H.M. Baskonus, L. Shi, New investigation of bats-hosts-reservoir-people coronavirus model and application to 2019-nCoV system, Adv. Differ. Equ. 2020 (2020) 391, https://doi.org/10.1186/s13662-020-02831-6.
[15] W. Gao, P. Veeresha, H.M. Baskonus, D.G. Prakasha, P. Kumar, A new study of unreported cases of 2019-nCOV epidemic outbreaks, Chaos, Solit. Fract. 138 (2020) 109929, https://doi.org/10.1016/j.chaos.2020.109929.
[16] E.F. Doungmo Goufo, Y. Khan, Q.A. Chaudhry, HIV and shifting epicenters for COVID-19, an alert for some countries, Chaos, Solit. Fract. 139 (2020) 110030.

[17] A. Atangana, Modelling the spread of COVID-19 with new fractal-fractional operators: Can the lockdown save mankind before vaccination?, Chaos, Solit Fract. 136 (2020) 109860, https://doi:10.1016/j.chaos.2020.109860.
[18] W. Gao, P. Veeresha, D.G. Prakasha, H.M. Baskonus, Novel dynamic structures of 2019-nCoV with nonlocal operator via powerful computational technique, Biology 9 (2020) 107, https://doi.org/10.3390/biology9050107.
[19] M. Higazy, Novel fractional order SIDARTHE mathematical model of the COVID-19 pandemic, Chaos, Solit. Fract. 138 (2020) 110007, https://doi.org/10.1016/j.chaos.2020.110007.
[20] G. Giordano, F. Blanchini, R. Bruno, P. Colaneri, A. Di Filippo, A. Di Matteo, M. Colaneri, Modelling the COVID-19 epidemic and implementation of population-wide interventions in Italy, Nat. Med. 22 (2020), https://doi.org/10.1038/s41591-020-0883-7.
[21] Biao Tang, XiaWang, Qian Li, Nicola Luigi Bragazzi, Sanyi Tang, Yanni Xiao, Jianhong Wu, Estimation of the transmission risk of the 2019-nCoV and its implication for public health interventions, J. Clin. Med. 9 (2020) 462. doi:10.3390/jcm9020462
[22] Esin Ilhan, I. Onur Kıymaz, A generalization of truncated M-fractional derivative and applications to fractional differential equations, Appl. Math. Nonlinear Sci. 5 (1) (2020) 171–188, https://doi.org/10.2478/amns.2020.1.00016.
[23] C. Cattani, A review on harmonic wavelets and their fractional extension, J. Adv. Eng. Comput. 2 (4) (2018) 224–238, https://doi.org/10.25073/jaec.201824.225.
[24] A.M. Yang, Y.Z. Zhang, C. Cattani, G.N. Xie, M.M. Rashidi, Y.J. Zhou, X.J. Yang, Application of local fractional series expansion method to solve Klein-Gordon equations on Cantor sets, Abstr. Appl. Anal. 2014 (2014), Article ID 372741.
[25] W. Gao, G. Yel, H.M. Baskonus, C. Cattani, Complex solitons in the conformable (2 + 1)(2 + 1)-dimensional Ablowitz–Kaup–Newell–Segur equation, AIMS Math. 5 (1) (2020) 507–521.
[26] J. Singh, D. Kumar, Z. Hammouch, A. Atangana, A fractional epidemiological model for computer viruses pertaining to a new fractional derivative, Appl. Math. Comput. 316 (2018) 504–515.
[27] W. Gao, P. Veeresha, D.G. Prakasha, H.M. Baskonus, G. Yel, New numerical results for the time-fractional Phi-four equation using a novel analytical approach, Symmetry 12 (2020), Article ID 478.
[28] H. Durur, O. Taşbozan, A. Kurt, M. Şenol, New wave solutions of time fractional Kadomtsev-Petviashvili equation arising in the evolution of nonlinear long waves of small amplitude, Erzincan Univ. J. Sci. Technol. 12 (2) (2019) 807–815.
[29] K.M. Owolabi, Z. Hammouch, Spatiotemporal patterns in the Belousov-Zhabotinskii reaction systems with Atangana-Baleanu fractional order derivative, Physica A 523 (2019) 1072–1090.
[30] A. Yokus, S. Gulbahar, Numerical solutions with linearization techniques of the fractional Harry Dym equation, Appl. Math. Nonlinear Sci. 4 (1) (2019) 35–42.
[31] D. Kumar, J. Singh, D. Baleanu, Analysis of regularized long-wave equation associated with a new fractional operator with Mittag-Leffler type kernel, Physica A 492 (2018) 155–167.
[32] H. Durur, O. Tasbozan, A. Kurt, New analytical solutions of conformable time fractional bad and good modified Boussinesq equations, Appl. Math. Nonlinear Sci. 5 (1) (2020) 447–454.
[33] X.J. Yang, F. Gao, A new technology for solving diffusion and heat equations, Therm. Sci. 21 (1 Part A) (2017) 133–140.
[34] J. Singh, D. Kumar, D. Baleanu, A new analysis of fractional fish farm model associated with Mittag-Leffler type kernel, Int. J. Biomathematics (2019), https://doi.org/10.1142/S1793524520500102.
[35] S. Kumar, A. Ahmadian, R. Kumar, D. Kumar, J. Singh, D. Baleanu, M. Salimi, An efficient numerical method for fractional sir epidemic model of infectious disease by using Bernstein wavelets, Mathematics 8 (2020) 558.
[36] D. Kumar, J. Singh, M. Al Qurashi, D. Baleanu, A new fractional SIRS-SI malaria disease model with application of vaccines, antimalarial drugs, and spraying, Adv. Differ. Equ. 2019 (2019) 278. doi: 10.1186/s13662-019-2199-9.
[37] N.H. Sweilam, S.M. Al-Mekhlafi, Optimal control for a nonlinear Mathematical model of tumor under immune suppression a numerical approach, Optimal Control Appl. Meth. 39 (2018) 1581–1596.
[38] N.H. Sweilam, S.M. Al-Mekhlafi, D. Baleanu, Optimal control for a fractional tuberculosis infection model including the impact of diabetes and resistant strains, J. Adv. Res. 17 (2019) 125–137.
[39] Saif Ullah, M.A. Khan, Modeling the impact of non-pharmaceutical interventions on the dynamics of novel coronavirus with optimal control analysis with a case study, Chaos, Solit. Fract. 139 (2020) 110075, https://doi.org/10.1016/j.chaos.2020.110075.
[40] H. Laarabi, A. Abta, K. Hattaf, Optimal Control of a delayed SIRS epidemic model with vaccination and treatment, Acta Biotheor 63 (15) (2015) 87–97.
[41] Ndolane Sene, SIR epidemic model with Mittag-Leffler fractional derivative, Chaos, Solit. Fract. 137 (2020) 109833. doi: 10.1016/j. chaos.2020.109833.
[42] Ndolane Sene Second-grade fluid model with Caputo-Liouville generalized fractional derivative, Chaos, Solit. Fract. 133 (2020) 109631. https://doi.org/10.1016/j.chaos.2020.109631.
[43] Ndolane Sene, Fractional diffusion equation with new fractional operator, Alexandria Eng. J. (2020), https://doi.org/10.1016/j.aej.2020.03.027.
[44] Melanie Mitchell, An Introduction to Genetic Algorithms, MIT Press, Cambridge, MA, 1996.
[45] M.A. Khan, The dynamics of a new chaotic system through the Caputo-Fabrizio and Atanagan-Baleanu fractional operators, Adv. Mech. Eng. 11 (7) (2019), 1687814019866540.
[46] M.U. Saleem, M. Farman, A. Ahmad et al., A Caputo Fabrizio fractional order model for control of glucose in insulin therapies for diabetes, Ain Shams Eng. J. doi: 10.1016/j.asej.2020.03.006.
[47] A.A. Kilbas, H.M. Srivastava, J.J. Trujillo, Theory and applications of fractional differential equations, vol. 204, North-Holland, Amsterdam, 2006.
[48] M. Caputo, M. Fabrizio, A new definition of fractional derivative without singular kernel, Prog. Fract. Differ. Appl. 1 (2015) 73–85.
[49] J. Singh, D. Kumar, D. Baleanu, On the analysis of fractional diabetes model with exponential law, Adv. Differ. Eqs. 2018 (2018) 231.
[50] J.J. Losada, J. Nieto, Properties of the new fractional derivative without singular kernel, Prog. Fract. Differ. Appl. 1 (2015) 8792.
[51] D. Boiroux, A.K. Duun-Henriksen, S. Schmidt, K. Nørgaard, N.K. Poulsen, H. Madsen, J.B. Jørgensen, Assessment of model predictive and adaptive glucose control strategies for people with type 1 diabetes, in: The 19th IFAC World Congress.
[52] World Health Organization (WHO), Novel Coronavirus-China, Disease Outbreak News: Update. Available online: https://www.who.int/csr/don/12-january-2020-novel-coronavirus-china/en/ (accessed on 23 January 2020).
[53] National Health Commission of the People's Republic of China. Available online: http://www.nhc.gov.cn/xcs/xxgzbd/gzbd_index.shtml (accessed on 23 January 2020).
[54] C. Castillo-Chavez, C.W. Castillo-Garsow, A. Yakubu, Mathematical models of isolation and quarantine, JAMA 290 (2003) 2876–2877.
[55] M. Gopal, Control Systems: Principles and Design, Tata McGraw-Hill Education, 2002.
[56] J.K. Hunter, B. Nachtergaele, Applied Analysis, World Scientific, Singapore, 2001.

Please cite this article in press as: M. Higazy, M.A. Alyami, New Caputo-Fabrizio fractional order $SEIAS_qE_qHR$ model for COVID-19 epidemic transmission with genetic algorithm based control strategy, Alexandria Eng. J. (2020), https://doi.org/10.1016/j.aej.2020.08.034

[57] K. Diethelm, N.J. ForD, A.D. Freed, Y. Luchko, Algorithms for the fractional calculus: a selection of numerical methods, Comput. Meth. Appl. Mech. Eng. 194 (6–8) (2005) 743–773.
[58] P. van den Driesschea, J. Wamough, Reproduction numbers and sub-threshold endemic equilibria for compartmental models of disease transmission, Math. Biosci. 180 (1-2) (2002) 29–48.
[59] AMS Mahdy, M Higazy, KA Gepreel, AAA El-dahdouh, Optimal control and bifurcation diagram for a model nonlinear fractional SIRC, Alexandria Engineering Journal (2020), https://doi.org/10.1016/j.aej.2020.05.028, In press.
[60] AMS Mahdy, N.H. Sweilam, M Higazy, Approximate solution for solving nonlinear fractional order smoking model, Alexandria Engineering Journal 59 (2) (2020) 739–752, https://doi.org/10.1016/j.aej.2020.01.049.
[61] K.A. Gepreel, M. Higazy, A.M.S. Mahdy, Optimal control, signal flow graph, and system electronic circuit realization for nonlinear *Anopheles* mosquito model, International Journal of Modern Physics C (2020), https://doi.org/10.1142/S0129183120501302.